

Heat integration between CO₂ Capture and Liquefaction and a CHP Plant

Impact on Electricity and District Heating Delivery at Renova's CHP Plant in Sävenäs

Master's thesis in Master Program Sustainable Energy Systems

CAROLINE HAMMAR

DEPARTMENT OF SPACE, EARTH AND ENVIRONMENT

CHALMERS UNIVERSITY OF TECHNOLOGY
Gothenburg, Sweden 2022
www.chalmers.se

MASTER'S THESIS 2022

Heat integration between CO₂ Capture and Liquefaction and a CHP Plant

Impact on Electricity and District Heating Delivery at Renova's
CHP Plant in Sävenäs

CAROLINE HAMMAR



CHALMERS
UNIVERSITY OF TECHNOLOGY

Department of Space, Earth and Environment
Division of Energy Technology
CHALMERS UNIVERSITY OF TECHNOLOGY
Gothenburg, Sweden 2022

Heat integration between CO₂ Capture and Liquefaction and a CHP Plant
Impact on Electricity and District Heating Delivery at Renova's CHP Plant in
Sävenäs
CAROLINE HAMMAR

© CAROLINE HAMMAR, 2022.

Supervisor: Lia Detterfelt, Renova
Supervisor: Johanna Beiron, Max Biermann and Sebastian Karlsson, Department
of Space, Earth and Environment
Examiner: Fredrik Normann, Department of Space, Earth and Environment

Master's Thesis 2022
Department of Space, Earth and Environment
Division of Energy technology
Chalmers University of Technology
SE-412 96 Gothenburg
Telephone +46 31 772 1000

Cover: Integration between Renova's WTE CHP plant in Sävenäs and a CO₂ capture
and liquefaction plant

Typeset in L^AT_EX
Printed by Chalmers Reproservice
Gothenburg, Sweden 2022

Heat integration between CO₂ Capture and Liquefaction and a CHP Plant
Impact on Electricity and District Heating Delivery at Renova's CHP Plant in
Sävenäs

CAROLINE HAMMAR

Department of Space earth and Environment
Chalmers University of Technology

Abstract

Carbon capture and storage (CCS) is an important technology for emissions difficult to mitigate with fuel-switching or electrification - like emissions from waste incineration. However, an installation of CO₂ capture to a combined heat and power (CHP) plant may result in a substantial decrease in electricity and district heating (DH) delivery. This thesis evaluates the effects on electricity and DH delivery of an integrated capture and liquefaction plant treating 60% of the flue gases from Renova's waste-to-energy (WTE) CHP plant in Sävenäs.

Two CO₂ absorption technologies, monoethanolamine (MEA) or hot potassium carbonate (HPC) based, are evaluated with respect to the practical constrains of the CHP plant. The heat integration evaluated possibilities for the heat extraction from the CHP plant to drive the capture plant, as well as the possibilities for recovery of heat from the capture and liquefaction to the district heating system in the CHP plant.

The work concludes that the CHP plant with an integration to a capture and liquefaction plant utilizing HPC deliver more DH compared to the current delivery without CCS implementation. However, HPC also entails a significant reduction in electricity delivery compared to current levels. The MEA based process delivers a similar amount DH as the current levels and has a lower electricity loss than the HPC process. CCS operation during the summer season requires an investment in additional cooling capacity of 28.3 MW for MEA and 23.2 MW for HPC. Therefore, it is recommended to perform an economic analysis of the option to solely operate the CCS plant during the winter season.

Furthermore, the work highlight the broad spectra of effects on the local energy system of a CCS integration - the resulting effect on electricity delivery was 48-88% of the retained electricity delivery and the resulting district heating delivery was 99-116% of the current delivery. The choice of solvent, heat source for solvent generation, level of CCS heat recovery, and possibility for heat pumping are all important aspects for the CCS integration.

Keywords: CCS, CHP, Waste-to-energy, Heat recovery

Sammanfattning

Koldioxidavskiljning och lagring (eng CCS) har föreslagits som en lösning till att minska CO₂-utsläppen och uppfylla Parisavtalet. Tidigare arbete om ämnet visar dock att en installation av CO₂ avskiljning och förvätskning till ett kraftvärmeverk leder till avsevärda förluster i el- och fjärrvärmeleverans om inte energiåtervinning implementeras. Det här projektet utvärderar därför påverkan på el- och fjärrvärmeleveransen när en avskiljnings- och förvätskningsanläggning värmeintegreras med kraftverket. I projektet antogs anläggning behandla 60% av rökgasflödet.

Integrationen utvärderades för Renovas avfallskraftvärmeverk (AKV) i Sävenäs med två olika CO₂-absorptionsmetoder som använder monoetanolamin (MEA) och hot potassium carbonate (HPC) som CO₂ absorbent. Värmeintegrationen utvärderade olika möjligheter för värmeutvinningen från kraftvärmeverket för att driva avskiljningsanläggningen. Den utvärderade även möjligheter till värmeåtervinning från avskiljnings- och förvätskningsanläggningen till fjärrvärmesystemet i AKV med målet att öka fjärrvärmeproduktionen.

Projektet visade att avfallskraftvärmeverket, integrerat till en avskiljnings- och förvätskningsanläggning med HPC baserad absorption resulterar i en högre fjärrvärmeleverans jämfört med nuvarande leverans från AKV utan infångning och förvätskning. HPC leder dock även till en omfattande minskning av elleverans jämfört med både nuvarande leverans från AKV och fallet med MEA. Vidare, resulterade MEA-fallet i en fjärrvärmeleverans liknande nuvarande leverans från AKV. Projektet visade även att det finns incitament att enbart driva avskiljnings- och förvätskningsanläggning under vinterhalvåret då sommar drift medför investeringskostnader i kylningsutrustning motsvarande 28.3 MW för MEA och 23.2 MW för HPC. En fullständig ekonomisk analys av avskiljnings- och förvätskningsanläggning krävs dock för att kunna utesluta sommar drift. Vidare, kräver även integreringen med HPC en större investering av värmeväxlare, 13-15 st, jämfört med integreringen till MEA som skrävver 10-11 st.

Sammanfattningsvis kom projektet fram till att kraftvärmeverket kan leverera 48-88% av den nuvarande elleveransen efter en integration till en infångnings- och förvätskningsanläggning. Den maximala leveransen uppnås genom MEA-baserade absorptionen som drivs med värme från en kombination av värmekällor i kraftvärmeverket och där en lägre framledningstemperatur av fjärrvärmen. Projektet kom även fram till att kraftvärmeverket kan leverera 99-116% av den nuvarande fjärrvärmeleveransen efter en integration där den maximala leverans uppnås genom HPC-baserad absorption som drivs med ånga från AKV och där en ny absorptionsvärmepump installerats till kraftvärmeverket.

Nyckelord: CCS, kraftverk, avfallskraftvärmeverk, energiåtervinning

Acknowledgements

I would like to thank my supervisor Lia Detterfelt who has provided interesting ideas and valuable input for both the work and the report through our bi-weekly meetings. I would also like to thank Jonas Axnér and Malin Bruhn who have always shown a big interest in the project and who have been available for discussions and provided insights regarding the operation of Renova's plant. Additionally, I would like to give a special thanks to Andreas Hellström, a member of the operational staff at Renova, who was kind enough to give me a tour of the plant at multiple occasions.

I would also like to give a big thanks to Johanna Beiron, Max Biermann and Sebastian Karlsson who has always been available for discussing all the problems I've faced, regardless if it's been about simulation problems in Epsilon, the pinch analysis or the report. They have also given helpful insights about the work in our weekly meetings and has helped to improve the report by providing a detailed commentary. Furthermore, I would like to thank my examiner Fredrik Normann for helpful discussions and for sharing insights about how to improve the work further to make it as great as it possibly can be.

Lastly, I would like to thank Max Biermann and Tharun Roshan Kumar for performing the simulations in Aspen and thus improving the quality of the work and giving me time to focus on the heat integration.

Caroline Hammar, Gothenburg, February 13, 2022



Contents

Abbreviations	xii
Nomenclature	xv
List of Figures	xvii
List of Tables	xxi
1 Introduction	1
1.1 Aim and Scope	2
2 Background	3
2.1 Renova's waste-to-energy plant	3
2.1.1 Combined heat and power plants	3
2.1.2 Process at site in Sävenäs	4
2.2 Carbon capture and liquefaction	6
2.2.1 Amine based absorption with MEA	7
2.2.2 Hot potassium carbonate based absorption	8
2.2.3 Liquefaction	9
2.3 Heat integration	10
2.3.0.1 Heat sources to drive CO ₂ capture	11
2.3.0.2 Heat sinks to recover heat	11
3 Method	13
3.1 Process data collection	14
3.2 Modelling of stand alone processes	14
3.2.1 CHP plant model	15
3.2.2 Carbon capture model	17
3.2.3 Liquefaction simulation	18
3.3 Modelling of integration to CHP plant heat sources and heat sinks . .	19
3.3.1 Integration to heat sources	20
3.3.2 Integration to heat sinks	22
3.3.3 Integration to power sources	25
3.4 Pinch analysis	25
3.5 Case simulation	26
3.6 Energy performance evaluation	28

4	Results and Discussion	31
4.1	Modelling of stand alone processes	31
4.1.1	CHP plant model validation	31
4.1.2	Heating and cooling demands of CO ₂ capture and liquefaction	33
4.2	Evaluation of integrations to CHP plant heat sources and heat sinks .	35
4.2.1	Estimation of heat sources	35
4.2.2	Using 40 bar steam as a reboiler heat source	36
4.2.3	Reboiler condensate utilization	37
4.2.4	Integration locations in the district heating system for heat transfer from coolers	38
4.2.5	Impact of combining integrations	39
4.3	Case simulation	39
4.3.1	Capture technologies and heat supply	40
4.3.2	Seasonal variation	42
4.3.3	Impact of DH return and supply temperature	44
4.3.4	Impact of increased heat pump capacity	45
4.4	Summarizing evaluation	47
5	Conclusion	49
	Bibliography	51
A	Design specification	I
B	Aspen PLUS simulation output	V
C	Estimation of power demand for air coolers	IX

Abbreviations

CCL CO₂ capture and liquefaction.

CCS carbon capture and storage.

CHP combined heat and power.

CO₂ carbon dioxide.

DH district heating.

GHG green house gas.

HPC hot potassium carbonate.

HX Heat exchanger.

IPCC Intergovernmental Panel on Climate Change.

MEA monoethanolamine.

NO_x nitrogen oxide.

O₂ oxygen.

SCR selective catalytic reformer.

SO_x sulphur oxide.

WTE waste-to-energy.

Nomenclature

ΔP_b	Pressure loss over bundle
ΔT_{lm}	Log-mean temperature difference
η_f	Fan efficiency
η_m	Motor efficiency
A	Heat transfer area
A_t	Tube area
$E_{DH,produced}$	District heating produced
$E_{DH,supplied}$	District heating supplied
$E_{el,produced}$	Electricity produced
$E_{el,supplied}$	Electricity supplied
E_{fuel}	Energy input from fuels
E_{import}	Imported energy
$E_{supplied}$	Energy supplied
$E_{waste\ input}$	Total energy input from waste
F_t	LMTD correction factor
N_b	No. of bundles
N_{bd}	banks/bundle
N_{bk}	tubes/bank
p_t	tube pitch
Q	Cooling duty
U	Overall heat transfer coefficient
u_f	Face velocity
W_f	Fan work

List of Figures

2.1	Process scheme of a basic steam cycle	4
2.2	A simplified schematic picture of Renova waste-to-energy plant	5
2.3	Flow sheet of the final steps in the flue gas treatment	6
2.4	Summary of CO ₂ capture technologies	7
2.5	A simplified process scheme for absorption carbon capture with monoethanolamine	7
2.6	A simplified process scheme for absorption carbon capture with hot potassium carbonate	9
2.7	A simplified process scheme for liquefaction of CO ₂ , adapted from [31]	10
2.8	The flow of heat between the integration of Renova's CHP plant and the CO ₂ capture and liquefaction plant	11
3.1	Flow sheet of the methodology	13
3.2	EBSILON®Professional model of Renova's CHP plant before a CO ₂ capture and liquefaction integration	15
3.3	Process scheme of the Renova's CHP plant with integration to the CO ₂ capture and liquefaction plant	20
3.4	Process scheme of the hot water system with the integration to the CO ₂ capture and liquefaction plant	21
3.5	Process scheme of the pressure reduction station	22
3.6	Prioritization scheme of utilization of the heat sources to fulfill the heat demand in the CO ₂ capture process	22
3.7	Simplified process scheme of the district heating cycle	23
3.8	Workflow of the integration between the CO ₂ capture and liquefaction (CCL) plant and the DH system	24
3.9	Example of a composite curve diagram	26
3.10	Flow sheet of the evaluated system in the pinch analysis	26
3.11	Flow sheet of the investigated cases	27
4.1	Turbine performance for different inlet mass flow collected from process data and from the Ebsilon model of Renova's CHP plant. The x-axis starts from 80°C	33
4.2	Hot composite curves of the cooling demand of the CO ₂ capture and liquefaction for the selected hour during winter operation	35
4.3	Hot composite curves of the cooling demand of the CO ₂ capture and liquefaction for the selected hour during summer operation	35

4.4	Distribution of district heating and electricity production out of the total production of DH and electricity, when 40 bar steam is expanded to 3.5 bar in a turbine or pressure reduction station. The heat demand in the reboiler corresponds to the MEA based CO ₂ absorption. The figures applies to the selected hour during winter operation	37
4.5	Distribution of district heating and electricity production out of the total production of DH and electricity, when the condensate from the reboiler corresponding the MEA based CO ₂ based absorption is returned directly to the steam cycle and when the condensate is used to heat the district heating system and then returned to the steam cycle. The figures applies to the selected hour during winter operation	38
4.6	Simplified process scheme of the district heating cycle with locations for integrations to the CO ₂ capture and liquefaction plant	39
4.7	Composite curves, according to Figure 3.10, of the district heating system integrated with the CO ₂ capture and liquefaction plant, utilizing MEA as solvent and with a reboiler heat supply from steam. The figure applies for the selected hour during winter operation . . .	41
4.8	Composite curves, according to Figure 3.10, of the district heating system integrated with the CO ₂ capture and liquefaction plant, utilizing HPC as solvent and with a reboiler heat supply from steam. The figure applies for the selected hour during winter operation . . .	42
4.9	Deviation in electricity and DH delivery compared to the delivery from Renova's CHP plant without the integration, when the CHP plant is integrated with the CO ₂ capture and liquefaction plant with MEA and HPC based absorption and with a reboiler heat supply from steam. The figure applies for the selected hour during winter and summer operation	43
4.10	Deviation in electricity and DH delivery compared to the delivery from Renova's CHP plant without the integration, when the CHP plant is integrated with the CO ₂ capture and liquefaction plant with MEA and HPC based absorption and with a reboiler heat supply from steam, for different DH temperatures. The figure applies to the selected hour during winter operation	45
4.11	Grand composite curves of the district heating system and the absorption heat pumps with an additional heat pump compared to the current operated capacity, when the CHP plant is integrated with the CO ₂ capture and liquefaction plant with MEA based absorption and with a reboiler heat supply from steam. The figure applies to the selected hour during winter operation	46
4.12	Deviation in electricity and DH delivery compared to the delivery from Renova's CHP plant without the integration, when the CHP plant is integrated with the CO ₂ capture and liquefaction plant with MEA and HPC based absorption and with a reboiler heat supply from steam, for different absorption heat pumps capacities. The figure applies to the selected hour during winter operation	46

4.13	Summary of the result from the case simulation, represented in electricity and district heating delivery. The reference refers to the delivery from the current CHP plant. The figure applies to the selected hour during winter operation	47
B.1	Aspen PLUS model of the simulated MEA process	V
B.2	Aspen PLUS model of the simulated HPC process	VI
B.3	Aspen PLUS model of the simulated compression and liquefaction process	VI

List of Tables

3.1	Selected design specifications for the winter simulation in Ebsilon . . .	16
3.2	Selected design specifications for the summer simulation in Ebsilon . . .	16
3.3	Flue gas input parameters for the capture process in Aspen, collected from process data for the selected hour during winter and summer operation	17
3.4	Selected design specifications for the capture processes in Aspen . . .	18
3.5	Assumed parameters for liquefaction for the selected hour during winter and summer operation	19
3.6	Assumed minimum temperature differences	20
3.7	Stream specifications of current cooling demands fulfilled by the district heating system	24
4.1	Simulated electricity and district heating production and water flow rate of selected streams collected from the Ebsilon model of Renova's CHP plant and from process data for the selected hour during winter and summer operation.	32
4.2	Reboiler duty and temperature target of the solvent for MEA based CO ₂ absorption and HPC based absorption for the selected hour during winter and summer operation	34
4.3	Share of the estimated available heat from the feed water, the hot water, the 3.5 bar steam and the 40 bar steam compared to the reboiler demand in MEA and HPC based absorption for the selected hour during winter and summer operation	36
4.4	Simulated performance parameters of Renova's CHP plant and the number of heat exchangers needed for the integration, when the CHP plant and CO ₂ capture and liquefaction plant is fully integrated. The integration is performed for MEA and HPC with reboiler heat supply from steam only and a combination of heat sources, for the selected hour during winter operation. The reference electricity and DH delivery before the integration is also presented	40
4.5	New cooling investment required for the CO ₂ capture and liquefaction plant, when the CHP plant is integrated with the capture and liquefaction plant with MEA and HPC based absorption and with a reboiler heat supply from steam. The table applies for the selected hour during summer operation	44

4.6	Energy performance of Renova’s CHP plant when the CHP plant is integrated with the CO ₂ capture and liquefaction plant with MEA and HPC based absorption and with a reboiler heat supply from steam and a combination of heat sources. The reference corresponds to the performance of the CHP without the integration. The reference case The table applies to the selected hour during summer and winter operation	48
A.1	Design specifications for the the winter simulation in EBSILON®Professional	I
A.2	Design specifications for the the summer simulation in EBSILON®Professional	II
A.3	Flue gas input composition for the capture process in Aspen, collected from process data for the selected hour during winter and summer operation	II
A.4	Design specifications for the capture processes in Aspen	III
B.1	Performance of the coolers in the CO ₂ capture and liquefaction plant utilizing MEA as absorber for summer and winter operation	VII
B.2	Performance of the coolers and one heater in the CO ₂ capture and liquefaction plant utilizing HPC as absorber for summer and winter operation	VII
C.1	Design specification of air cooler	IX

1

Introduction

The Paris agreement states that the global temperatures should not exceed 2 °C compared to the pre-industrial levels and that efforts to limit the global temperature rise below 1.5 °C should be performed as it decreases the risks and impacts of climate change [1]. The Paris Agreement also states that all parties should strive to formulate a long-term climate strategy [1]. This strategy was in Sweden established by the Swedish government and states that Sweden will fulfil the goals of the agreement by achieving net zero emissions by Year 2045 and negative emission thereafter [2]. One of the technologies suggested both by the Swedish government and the Intergovernmental Panel on Climate Change (IPCC) to reduce green house gas (GHG) emission is carbon capture and storage (CCS) [2, 3]. CCS is a technology where carbon dioxide, from large-emitting point sources, are concentrated, compressed and transported to a long term storage location to mitigate CO₂ emissions. CCS also has the possibility to achieve negative emission by capturing emissions from biogenic energy sources [3].

Implementation of CCS may be useful for many industry sectors to fulfil the climate goals [4], one of these are the waste management sector, in particular the waste-to-energy (WTE) plants. WTE plants produce heat and/or electricity by using municipal solid waste as fuel [5]. The need to capture carbon dioxide (CO₂) from this process arise due to the composition of waste [5], which is partly fossil based [6]. Additionally, an implementation of CCS at a WTE plant will open opportunities for negative emissions if more than the fossil share of the carbon dioxide is captured. Even though waste, both to quantity and its composition, may change over the years, WTE plants could still be essential for waste management [7], which underlines the interest for CCS implementation.

One WTE plants, which will be investigated in this master thesis, is the WTE plant in Sävenäs, Gothenburg operated and owned by Renova AB. A report by Andersson regarding carbon capture technologies at Sävenäs WTE plant [8], suggested post-combustion capture, utilizing MEA solution as capture technology since this technology was well tested at the time and resulted in a low cooling demand which is of limited access at the plant [8]. However, with the recent success of Stockholm Exergi to utilize hot potassium carbonate (HPC) as sorbent in a test plant for carbon capture at their combined heat and power (CHP) plant [9], both of these capture technologies might be of interest at Renova's WTE plant.

Andersson [8] concluded that an implementation of carbon capture and liquefaction

(CCL) could result in a decrease in the total energy delivery of electricity and district heating (DH) by one third compared to current levels. The report also suggests measures to decrease the losses in energy delivery by implementing heat recovery to the CCL plant and integrate it with the rest of the facility [8].

The heat integration between the CHP plant and CCL process will focus on the heat extracted from the CHP plant to fulfill the heat demand in the CCL process, which depending on the heat source will affect the performance of the plant. It will also focus on the heat ejected from the CCL plant, which has potential to contribute to the production of DH.

The extent of the heat integration will depend on the temperature levels of the CCL process and the temperature levels in the integration locations in the CHP plant such as the DH system, since heat will be transferred between these processes to cool and heat each other. A cooling demand in the CCL plant at low temperature will thus be hard to integrate with the DH system which is limited by a minimum temperature. An adjustment of the temperature profile of the DH system could thus increase the potential for integration and the performance of the CHP.

1.1 Aim and Scope

This master thesis studies the compatibility of MEA and HPC based CO₂ absorption at Renova's WTE plant. The aim is to compare opportunities for heat integration between the CHP plant and the CO₂ capture and liquefaction installation by quantifying the impact on electricity and DH deliveries as well as cooling demand. The evaluation considers the operational constraints of the CHP plant as well as different supply and return district heating water temperatures.

The CCL installation of is performed in connection to the installation of two new furnaces planned for Year 2030. The new furnaces are of the same size and operate similarly as two of the current furnaces, called Furnace 4 and Furnace 5. The capture and liquefaction unit will be designed to capture CO₂ from the flue gas solely from these two furnaces, which corresponds to 60% of the total flue gas and 115 ktonCO₂/year. Furthermore, the new installations will have the same flue gas treatment as the current Furnace 7 which has additional cleaning units compared to Furnace 4 and 5

2

Background

This chapter focuses on three main subjects: Renova's WTE plant, carbon capture and liquefaction and the heat integration. The first part describes the operation of different units in a generic CHP plant and Renova's WTE plant in particular. The second subject describes the theory behind CCL. The last subject describes the energy flow between the CHP plant and the CCL plant as well as locations of interest for the integration.

2.1 Renova's waste-to-energy plant

Renova's WTE plant in Sävenäs burns waste from the owner municipalities Ale, Göteborg, Härryda, Kungälv, Lerum, Mölndal, Partille, Stenungsund, Tjörn och Öckerö for production of electricity and district heating. The delivered electricity and district heat from the plant corresponds to 30% respective 5% of the local heat demand and electricity demand. The following sections will describe how electricity and DH is produced in a general CHP as well as site specific details about Renova's plant.

2.1.1 Combined heat and power plants

A combined heat and power system produce power and useful heat simultaneously in one energy conversion plant [10]. This master thesis focuses on a steam-based CHP plant since this system is utilised at Renova's WTE plant. A basic steam cycle consists of four units: boiler, steam turbine, condenser and pump [10, 11], which is presented in Figure 2.1.

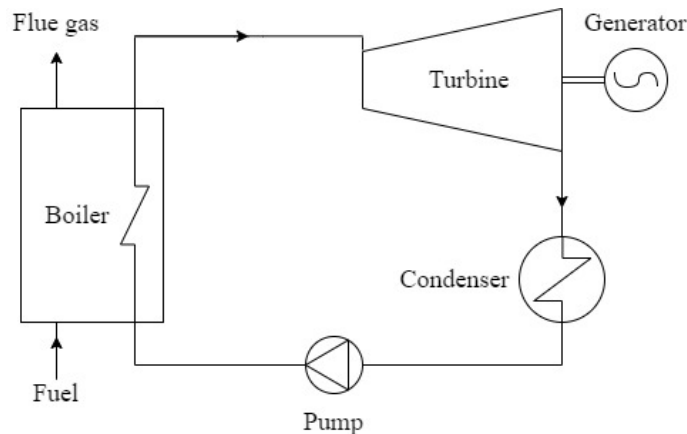


Figure 2.1: Process scheme of a basic steam cycle

In the steam cycle, superheated, high pressure steam generated in the boiler is expanded in the steam turbine to low pressure steam [10, 11]. The generator connected to the turbine produce power from the work performed by the expansion of steam. The low pressure steam is then condensed in the condenser which utilizes the heat of condensation for district heating production [11]. The feed water pump increases the pressure of the feed water leaving the condenser and supplies it to the boiler where it is converted to superheated steam with heat transfer from fuel combustion [10, 11].

2.1.2 Process at site in Sävenäs

Renova has permission to manage 550 000 tonne waste per year [12]. On average, 60% of the delivered waste is bio-based material and 40% is fossil-based material which means that the majority of the produced CO₂ from waste incineration does not provide to the net contribution of CO₂ to the atmosphere [13].

The WTE plant is operated without interruptions to provide heat and electricity to the residents of Gothenburg. During the summer period when the demand for heat is low, the plant is operated at part load to save fuel, i.e. waste, for the winter period when the demand is high. The furnaces are therefore stopped one at a time for maintenance work during the summer [12].

A simplified schematic picture of Renova's WTE plant is presented in Figure 2.2. The following information regarding operation and specific units in the plant was collected from Renova's internal information system as well as staff. The plant consists of four furnaces called "Furnace 1", "Furnace 4", "Furnace 5" and "Furnace 7", where each furnace has its separate flue gas treatment system called a flue gas treatment line, which has been simplified in Figure 2.2.

The steam cycle, which is represented by the blue and red line in Figure 2.2, produces electricity and DH as described for a general CHP plant. The turbine has an extraction at 3.5 bar and an outlet pressure of 1.1-1.2 bar. The 3.5 bar steam is distributed in a 3.5 bar system which mainly powers absorption heat pumps at

the plant. Furthermore, some of the 3.5 bar steam is used to preheat the feed water and as pressure regulation in the feed water tanks. The low pressure steam, 1 bar steam, is condensed in the condenser to provide heat for the DH system. The plant is also equipped with two sets of feed water pumps, one set is powered by electricity and one set is powered by a steam turbine utilizing high pressure steam.

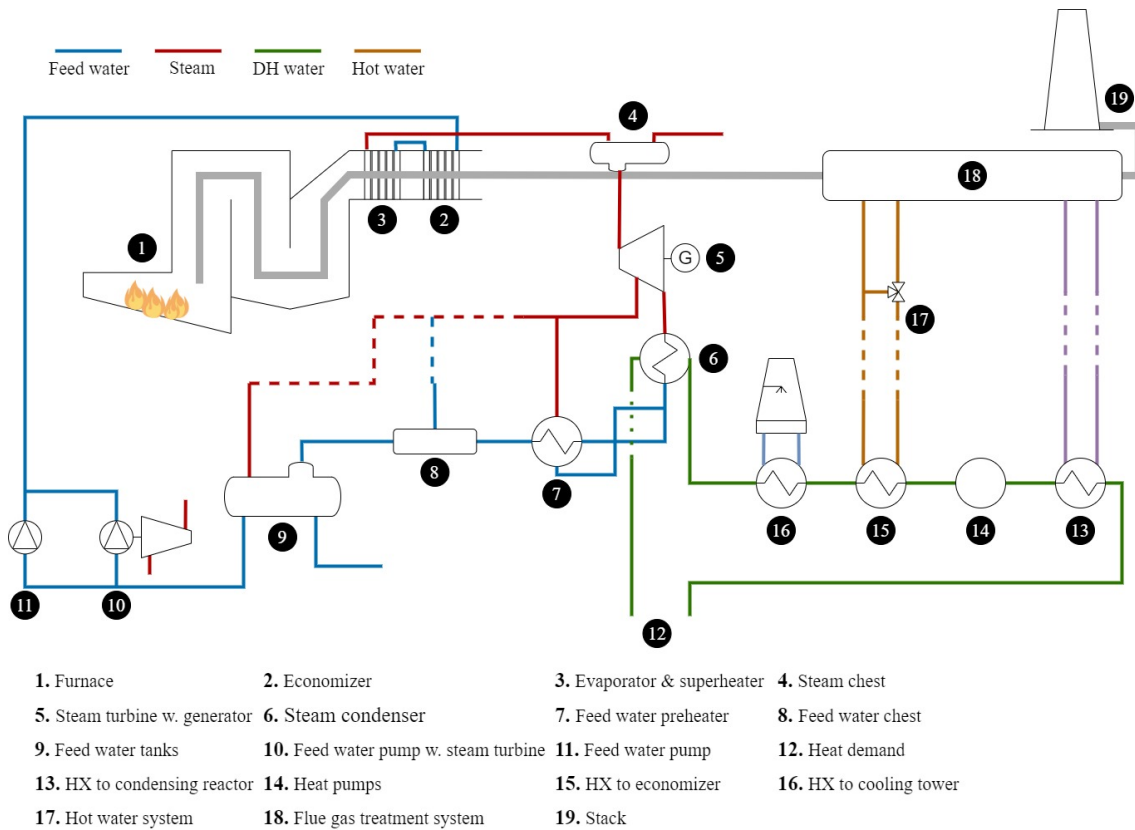


Figure 2.2: A simplified schematic picture of Renova waste-to-energy plant

The DH system, represented by the green line in Figure 2.2 mainly extracts heat from the steam condenser. Some heat is also extracted from a condensing reactor located in the flue gas treatment, the absorption heat pumps and a cycle called the "hot water system" which extracts heat from the flue gases in an economizer. Lastly, the DH system is connected to cooling towers which transfer excess heat to the air during the summer period.

Another important system is the flue gas treatment. The main purpose of this system is to wash out pollutants from the flue gas and to recover energy. The process is initiated with an electrostatic precipitator where particles are removed. Heat is then recovered to the hot water system in the economizer followed by a wet scrubber system that washes out metals, hydrochlorides and Sulphur. The final steps of the flue gas treatment system differs between the four flue gas treatment lines depending on when they were installed. Since the new installation will be most similar to the treatment line of Furnace 7, this is the system in the focus in this work. A schematic picture of the last steps in the flue gas treatment line of furnace 7 is presented in

Figure 2.3.

The last steps of this system is equipped with a wet electrostatic precipitator which removes aerosols. The flue gas is then cooled by water in the condensation reactor. The last step is a selective catalytic reformer (SCR) where nitrogen oxide (NO_x) is removed before the flue gas is ejected to the stack. Figure 2.3 shows that cold flue gas from the condensation reactor is heated with hot flue gas from the SCR, since the SCR requires a higher temperature.

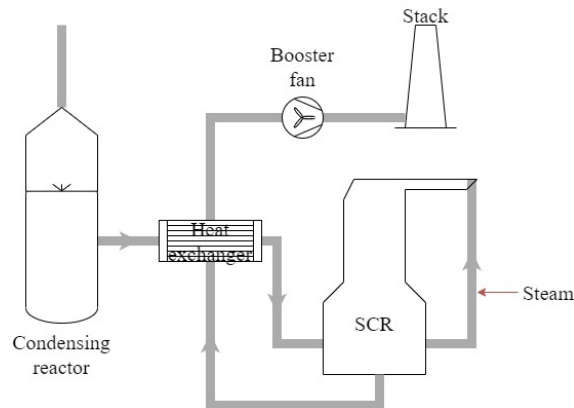


Figure 2.3: Flow sheet of the final steps in the flue gas treatment

2.2 Carbon capture and liquefaction

Carbon capture and liquefaction are two steps in the carbon capture and storage process. The remaining steps include transportation of CO_2 from the capture site and the storage process to a permanent storage location [3].

Carbon capture technologies can be divided into three different groups: pre-combustion capture, oxyfuel capture and post-combustion capture. Since pre-combustion and oxyfuel capture are implemented before combustion, these are unsuitable to retrofit into an existing plant [14], and will thus be unsuitable to integrate to Renova's WTE plant. Post-combustion will therefore be investigated further in this master thesis.

Post-combustion capture is divided into multiple categories. According to Andersson [8], who previously investigated applicable post-combustion technologies to Renova's WTE plant, absorption is the most viable of post-combustion technologies for Renova [8]. The absorption process captures carbon dioxide by reacting CO_2 with a sorbent in a water solution which will convert CO_2 from gas phase to liquid phase [15].

Andersson concluded that amine-based absorption with monoethanolamine (MEA) is more suitable compared to ammonia-based absorption for Renova's WTE plant due to the need for cooling in the latter technology and the limited access to cooling water at the plant [8]. A third absorption technology, hot potassium based ab-

sorption, has also become viable for integration with CHP plants after the success of Stockholm Exergi's test plant which utilize this technology [9]. A summary of the mentioned carbon capture technologies is presented in Figure 2.4. Since amine based and HPC based absorption was considered viable for Renova's WTE plant, these are investigated in this thesis and is described in more detail in the following sections.

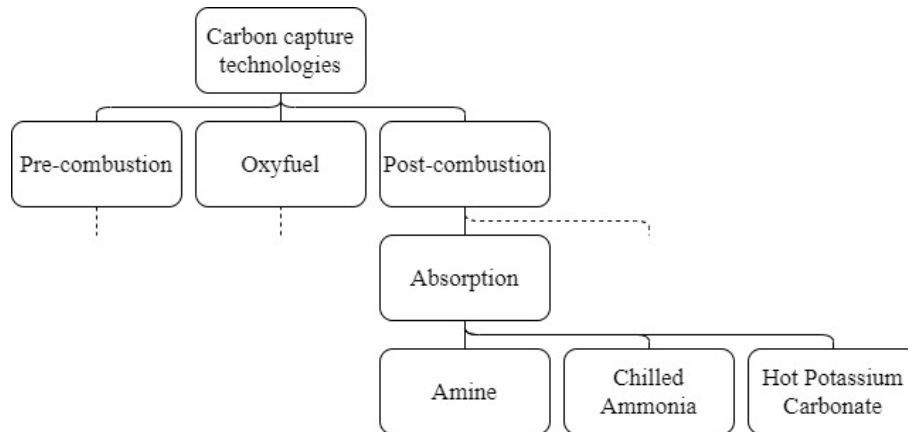


Figure 2.4: Summary of CO₂ capture technologies

2.2.1 Amine based absorption with MEA

MEA is a well-proven CO₂ absorbent and has been used for decades to remove CO₂ from natural gas with chemical absorption [16]. The advantage of MEA is its high reactivity which results in a high absorption rate and thus high CO₂ removal rate. The major drawbacks of absorption with MEA is the energy requirement for the regeneration of solvent entailed by the high temperatures and high heat of reaction. MEA is also sensitive to high levels of sulphur oxide (SO_x) and oxygen (O₂) in the flue gas which may cause solvent degradation. Lastly, MEA is corrosive at higher concentration which may cause damage to the equipment [17]. A general absorption carbon capture process utilizing MEA as solvent is shown in Figure 2.5

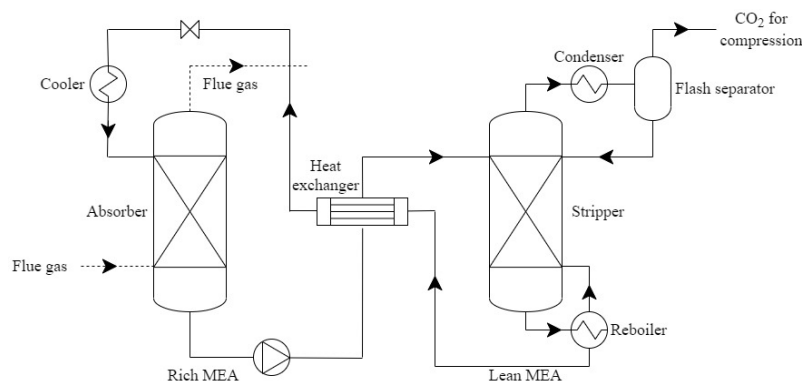


Figure 2.5: A simplified process scheme for absorption carbon capture with monoethanolamine

In the CO₂ absorption process, the flue gas enters at the bottom of the absorption

column while the MEA solvent, called lean solvent due to the low CO₂ loading, enters at the top, in a counter current flow [18]. The lean solvent generally has a temperature of 40 to 60°C [3, 17, 19] and contains 30 wt% MEA [17, 20]. The absorption column operates at 1 bar [21]. The contact from the counter flow between the two streams results in the absorption of carbon dioxide in the MEA solution [18]. Capture rate is usually set to 90% of the CO₂ in the flue gas due to the high equipment costs for higher absorption rates [22]. The solution with absorbed carbon dioxide, called rich solvent, is pumped to the top the desorption column, also called stripper. The process scheme in Figure 2.5 can be modified with a washer which is installed on top of the absorber to remove entrained MEA in the flue gases with water [17].

The desorption of CO₂ is also performed with a counter current flow, with the rich solvent entering at the top of the stripper and steam generated in the reboiler at the bottom of the column [18]. The rich solvent enters at 100 to 140°C [17, 19, 20] and the stripper operates at 1.2-2.5 bar [17, 19, 21]. The heat from the rising steam causes CO₂ to be released from the solvent to the gas phase which exits the column at the top with the remaining steam. The gas mixture is then cooled and the condensed steam is directed back to the desorption column as a reflux. Lean solvent exits the stripper at the bottom and is circulated back to the absorption column. Due to its high temperature, the lean solvent is used to heat the rich solvent. Additional cooling may be needed before the lean solvent enters the absorber again [18]. The MEA based capture process is thus driven by the heat supplied in the reboiler as well as the cooling.

2.2.2 Hot potassium carbonate based absorption

HPC based carbon dioxide absorption originated from the Benfield process developed 1950 which absorbs CO₂ from synthesis gas [23]. The advantages with HPC based absorption is the lower demand for solvent regeneration compared to MEA based absorption. Potassium carbonate also has a lower toxicity and lower cost compared to MEA. Furthermore, HPC is resistant to absorption degradation in the presences of O₂, SO_x and NO_x which may be present in the flue gases [23]. The main disadvantage of HPC based absorption is the extensive need for electricity to compress flue gas streams to elevated pressure conditions [24]. HPC also has a low reactivity with CO₂ which means that rate promoters and catalysts are often needed to improve the reaction rate and to reduce equipment size [23]. A general absorption carbon capture process utilizing HPC as solvent is shown in Figure 2.6

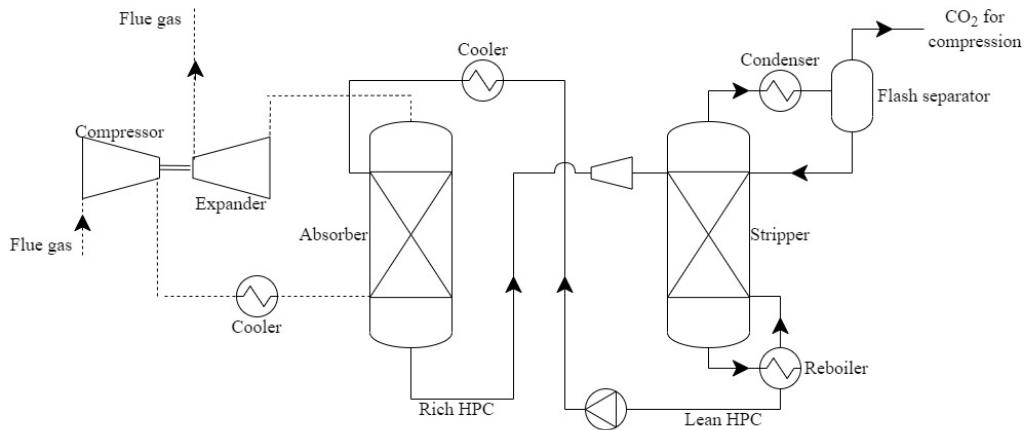


Figure 2.6: A simplified process scheme for absorption carbon capture with hot potassium carbonate

As shown in Figure 2.6, the major layout of the process is similar to the MEA based absorption. The flue gas entering the system is compressed and cooled to 6-15 bar [24–26] and 110°C [24, 26]. The compressed flue gas enters the absorber at the bottom while the lean solvent enters at the top at 6-15 bar and 50-80°C [24, 25]. The outgoing flue gas and rich solvent is expanded to atmospheric pressure before entering the stack and desorption column respectively. The flue gas expander is used to drive the flue gas compressor, seen in Figure 2.6, [25] The rich solvent enters the stripper at a temperature of 100-130°C. [24–26]

Absorption based carbon capture with HPC uses a pressure-swing to concentrate CO₂ corresponding the temperature-swing necessary to release CO₂ in absorption with MEA [25]. This generally results in a higher demand for electricity for compression with HPC compared to MEA, while the demand for regeneration heat is lower. [24]

2.2.3 Liquefaction

The treatment of the CO₂ stream leaving the absorption process depends on the means of transportation to the storage site [27]. CINFRACAP, a project aimed at investigating the possibilities for shared CO₂ transportation infrastructure in Gothenburg, concluded that the most suitable option for Renova would be to transport the CO₂ by truck from the WTE plant to the port of Gothenburg and then by ship to a long-term storage location. The carbon dioxide typically has to be compressed and liquefied to 15-17 bar and (-25)-(-30)°C for such transportation [28, 29].

There are two commercial liquefaction processes available, the first one use high pressure compression with free liquid expansion to liquefy CO₂, the second one use low pressure compression with an external refrigeration system. The second process is often preferred due to its lower energy cost [30] and is therefore the considered process in this project. A process scheme of the liquefaction process with an external

2. Background

refrigeration system is presented in Figure 2.7.

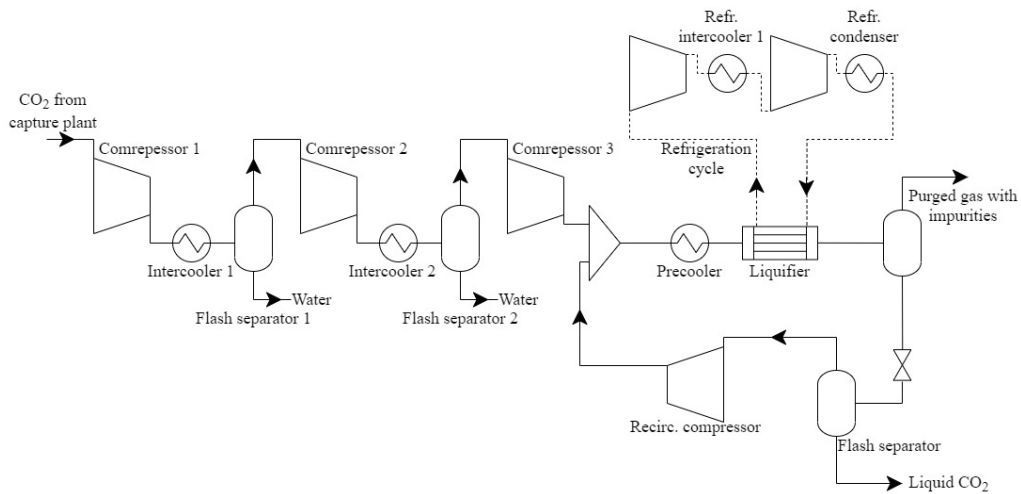


Figure 2.7: A simplified process scheme for liquefaction of CO₂, adapted from [31]

The first part of the liquefaction process is a compression train containing two to four stages of compression with intermediate cooling. The intercooler condenses steam and cools the carbon dioxide. The steam is then separated from the CO₂ in a flash separator [30, 31]. The stream is then cooled and liquefied with a refrigeration cycle using a refrigerant, such as ammonia, which in turn is compressed and cooled in a two stage vapor compression cycle. Lastly, the CO₂ stream enters a flash separator which separates liquid and gaseous CO₂, the gaseous CO₂ is recycled to the process. [31].

2.3 Heat integration

The heat integration between the WTE plant and the CCL plant focus on two aspects: the heat demand in the reboiler and the heat leaving the capture and liquefaction process. The first, involves a heat integration with the steam cycle and other hot systems in the CHP plant to fulfill the demand in the reboiler while the second involves heat integration with the DH cycle to recover more heat and increase the delivered DH. A figure of the heat flow in the heat integration is presented in Figure 2.8

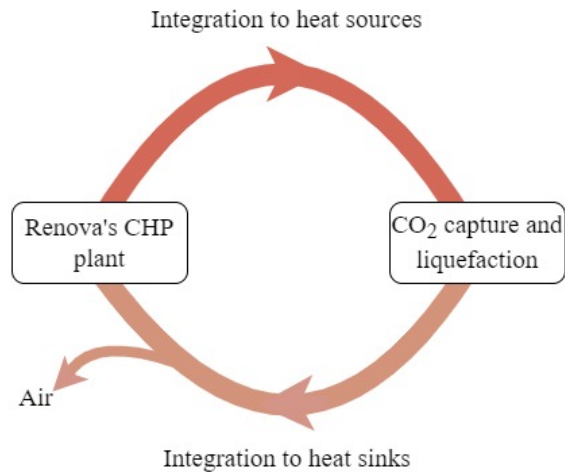


Figure 2.8: The flow of heat between the integration of Renova's CHP plant and the CO₂ capture and liquefaction plant

2.3.0.1 Heat sources to drive CO₂ capture

High temperature heat sources are available at multiple locations in the WTE plant, three of which has a temperature above 120°C. The first is the feed water entering the boiler which has a temperature of 140°C. The second, is the hot water system with a maximum temperature of 135°C. The purpose of the system is to cool the flue gas and deliver heat to the DH system.

Furthermore, there is the steam system which consists of 40, 3.5 and 1.1 bar steam where the 40 bar and 3.5 bar steam has a temperature above 120°. With the current operation, 40 bar steam is produced in the boiler while 3.5 bar steam is extracted from the turbine. The extraction of 3.5 bar steam is limited to 27 kg/s according to the manufacturer of the turbine, but other systems are installed that can provide additional 3.5 bar steam, such as a pressure reduction station, where 40 bar steam is expanded to 3.5 bar with a throttle and attemperated with feed water.

The available heat from the feed water, hot water system and 3.5 bar steam is limited due to constraints in the plant. A combination of multiple heat sources may therefore be necessary to fulfill the heat demand in the reboiler. To utilize 40 bar steam in the reboiler is the least favourable option due to the importance of this steam in the steam cycle for electricity generation. However, the heat content in the total 40 bar steam is enough to fulfill the total demand in the reboiler. 40 bar is thus suitable to use when heat from the feed water, hot water and 3.5 bar steam is insufficient.

2.3.0.2 Heat sinks to recover heat

The plant is equipped with several cooling systems, some involve cooling with water from the local river, while others involve cooling installations such as wet cooling towers. According to operational staff, cooling water from the river is currently utilized at the maximum capacity during the summer. Spare cooling capacity is also

limited from the cooling towers during the summer. Thus, an installation of CCL that increases the cooling demand requires a new cooling arrangement.

An option is to cool parts of the CCL process towards the DH cycle. The available cooling capacity of the DH cycle will depend on the operation of the heat pumps and heat exchangers which are currently cooled with the system and the temperature of the returning water which varies depending on season. Another option is to install new cooling systems. The most viable cooling options for a new installation is either to equip the carbon capture and liquefaction plant with air fans which will cool the process directly towards the ambient temperature, or to use a pipeline from the port of Gothenburg to cool the plant with sea water. Due to the difficulty of gaining permission to use sea water, air cooling was considered most favorable as a cooling investment for the CCL process.

The cooling arrangement for the CCL process will thus consist of cooling towards the DH cycle and cooling towards air. The arrangement between these will depend on the season and the situation for the DH system.

3

Method

This chapter describes the method applied in the project. A schematic picture of the methodology is presented in Figure 3.1. The project was initiated with a process data collection of Renova's plant from on-site studies. Information of the plant and its operational constraints was then used to create and simulate a model of Renova's CHP plant in EBSILON®Professional. From the data collection was also information about the flue gas conditions used for the simulation of the CO₂ capture and liquefaction which was simulated in Aspen PLUS®. These steps resulted in a validated model of Renova's plant and the heating, cooling and power demands of the capture and liquefaction plant.

Single integrations between the CCL plant and specific heat sources and heat sinks were then modelled by adding the demands from the Aspen simulations to the model of Renova's plant. The purpose of initially simulating single integrations was to quantify how much heat can be transferred in that specific integration and to evaluate how it should be transferred. Further on, the fully integrated systems, including all single integration was modelled. The fully integrated systems was also verified with a pinch analysis to ensure feasible heat transfer. Lastly the integrated systems was simulated in cases by adjusting the design specifications of the CHP model to fit the cases.

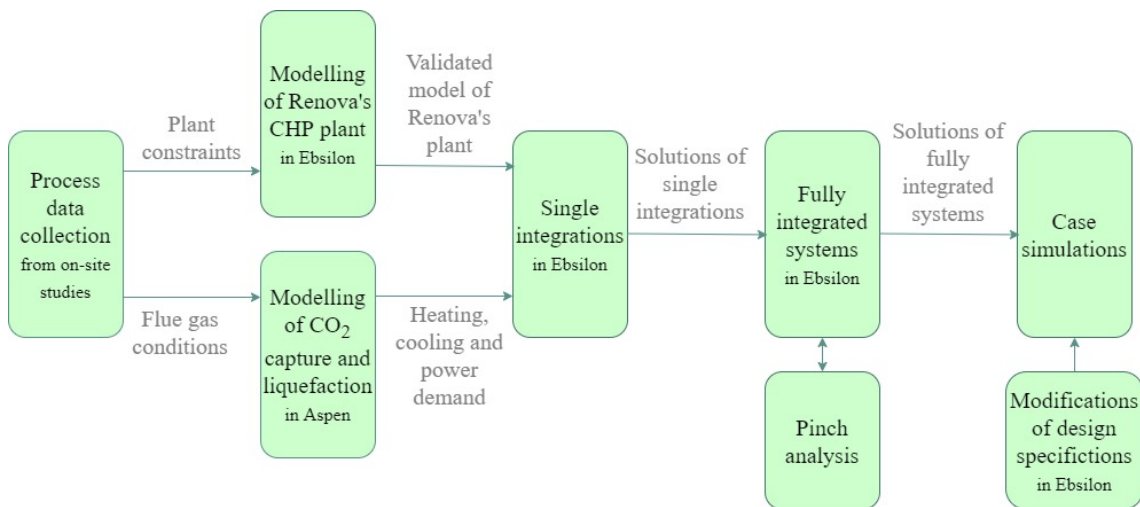


Figure 3.1: Flow sheet of the methodology

3.1 Process data collection

The plant data was collected in two ways, by a study of process schemes to map the flows within the plant. Secondly, by an onsite walkthrough with the operational staff which aimed to investigate important data point in further detail and to gain knowledge about operational guidelines. The process data of the plant was then gathered from Renova's internal data handling system, which collects both live data and historical trends. Extracted data included temperature and pressure levels, mass and volume flows, device specifications and heat and electricity production.

The general operational situation of the plant in 2030 was assumed to be equal to the present situation and process data from 2020 was extracted to describe the system. Regarding the properties of the flue gas entering the CCL process, the flow rate was assumed to equal the measured level Year 2020 from Furnace 4 and 5 while the temperature, pressure and flue gas composition was based on the Furnace 7, since this flue gas line is more similar to the intended new installations.

Furthermore, two operational points was chosen for the simulation of the systems, one during the summer and one during the winter. The summer operational point was based on 7th of June 12 o'clock, which is during the maintenance stop of Furnace 1 and before the stops of Furnace 4, 5 and 7. The reason why this was important is because the maintenance work usually alters the efficiency of the furnace which will be regained after a couple of months. The winter data point was set to 7th of December 12 o'clock. Data was extracted as hourly averages rather than averages of longer periods, this requires the data to be selected carefully to achieve a representative process description but will on the other hand avoid deviations in mass and energy balances.

3.2 Modelling of stand alone processes

This section describes the simulation of the WTE plant, carbon capture process and the liquefaction process in EBSILON®Professional and Aspen PLUS®. The benefit of initially simulating the systems separately was to be able to validate the Ebsilon model of Renova's CHP plant against process data and to be able to simulate the CHP plant and CCL plant with different tools. The benefit of using different tools arise due to the different areas of application of the simulation softwares which makes some tools more accurate and easy to use for some situations.

Ebsilon is mainly used for thermodynamic cycle processes by allowing the user to create systems by connecting prefabricated components, eg. turbines, condensers and steam generators, to each other. The system is then solved by algorithm equations from each component [32]. Aspen is used for simulation of chemical processes and can simulate reactions with chemicals, polymers and solids. [33]. Similar to Ebsilon is the system defined by the user with prefabricated components. The software then calculates the performance of the system by solving each component individually

and iteratively until the whole system converges.

3.2.1 CHP plant model

Renova's WTE plant was modelled in Ebsilon by the main parts of the steam cycle, the DH cycle and the hot water cycle, see Figure 2.2. The remaining systems such as the cooling systems were not included in the model since their interaction with the CCL process was considered negligible. The flue gas treatment was not included either since its interaction with the CCL plant is already accounted for in the simulation in Aspen. In addition, some parts of the steam cycle were simplified such as the system for the extracted steam which in reality is used for heat, pressure regulation and to power the absorption heat pumps, but is in the model represented as a heat consumer. The flowsheet of the WTE plant can be seen in Figure 3.2. Electricity production from the CHP plant is represented by the output from the generator and the district heating production is represented by the heat consumed in the DH consumer in Figure 3.2

The load of the steam cycle is in the model controlled by the waste input which is determined by the capacity of the furnaces and Renova's permission to incinerate waste on annual basis. The specific waste input therefore kept constant for each season for all simulations including simulation with heat integrations.

The winter and summer operation cases were simulated with a design and off-design mode in Ebsilon. The winter operation, when the plant operates at full capacity, was simulated in the design mode while the summer operation, when the plant is operated at part load due to the maintenance stop of one of the furnaces, was simulated in off-design mode.

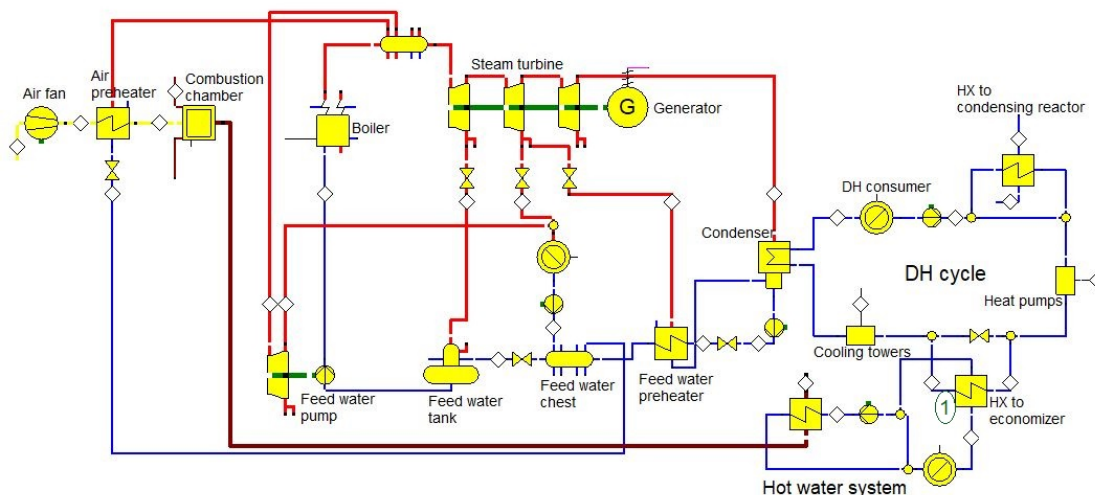


Figure 3.2: EBSILON®Professional model of Renova's CHP plant before a CO₂ capture and liquefaction integration

Selected design specifications for the model in the winter case are summarised in

3. Method

Table 3.1. The majority of the input is based on the process data collection at Renova. The composition of waste is based on another WTE plant called Lilljesjöverket, which is operated by Uddevalla Energi, and is assumed to have equivalent fuel input.

Table 3.1: Selected design specifications for the winter simulation in Ebsilon

	Value	Unit
Waste properties		
Waste consumption	17.54	[kg/s]
Furnace		
Air inlet conditions	30, 1.01	[°C], [bar]
Exit flue gas temperature	230	[°C]
Steam cycle		
Primary steam conditions	400, 40	[°C], [bar]
Steam turbine extraction 1 pressure	3.6	[bar]
Steam turbine extraction 2 pressure and flow rate	3.5, 13.9	[bar], [kg/s]
Steam turbine outlet pressure	1.11	[bar]
DH cycle		
Supply temperature	98.7	[°C]
Returned water temperature	38.9	[°C]
HX to economizer outlet temperature (noted as 1 in Figure 3.2)	73.6	[°C]
Hot water cycle		
Flow rate through economizer (water side)	120	[kg/s]
Economizer outlet temperature (flue gas side)	150	[°C]

For the summer model, some parameters were changed compared to the winter simulation. Assumptions for the summer case is summarized in table 3.2. A complete presentation of the design parameters for the models are summarised in Appendix A.

Table 3.2: Selected design specifications for the summer simulation in Ebsilon

	Value	Unit
Furnace		
Waste consumption	13.39	[kg/s]
Steam cycle		
Steam turbine extraction 2 flow rate	14.8	[kg/s]
DH cycle		
Supply temperature	103.7	[°C]
Returned water temperature	49.8	[°C]
HX to economizer outlet temperature	77.48	[°C]

The models for winter and summer operation were validated by comparing simulated electricity and DH output with reference process data. Mass and volumetric flow

rated were also compared with process data for the feed water entering the boiler, total DH water and the outgoing feed water from the preheater. In addition, the performance of the steam turbine was validated with process data. The validated models for summer and winter operation were further used for two purposes: as references of the performance before the CCL integration and as a starting point for simulations with a CCL integration.

3.2.2 Carbon capture model

The carbon capture processes were simulated in Aspen with a model setup by Gardarsdóttir et al. and Biermann et al. [34, 35] for the MEA based absorption and a model setup by Ochieng et al, Borhani et al. and Mumford et al. [36–38] with performance guidelines from Devries and Rochelle et al. [39, 40] for the HPC based absorption. The model set-ups in Aspen Plus is presented in Appendix B.

The flue gas input to the capture process is presented in Table 3.3. The flue gas input is collected from process data at the location the flue gas is collected from Furnace 4 and 5. The flue gas in Table 3.3 correspond to about 60% of the total flue gas volume flow from the plant. The capture plant is assumed to be located before heat exchanger to the SCR, according to Figure 2.3. This location was chosen due to its low temperature, which is beneficial to the efficiency of the amine absorption process. Also, the positioning downstream of the flue gas condensation guarantees low levels of impurities such as SO₂ [41, 42]. The composition of the incoming flue gas is based on measured levels in the WTE plant and is presented in Appendix A collected from process data for the selected hour during winter and summer operation

Table 3.3: Flue gas input parameters for the capture process in Aspen, collected from process data for the selected hour during winter and summer operation

	Winter	Summer	Unit
Pressure	1.01	1.01	[bar]
Temperature	31.7	44.4	[°C]
Volume flow	205 205	196 466	[m ³ /h]
CO ₂ -flow	10.83	9.90	[kg/s]

Both Aspen models used rate-based modelling for the absorber and desorber. Thermodynamic modelling was performed with ENRTL-RK for the MEA based process and ELECNRTL for the HPC based process. Selected design parameters for the models is summarised in Table 3.4, a complete presentation of the parameters can be seen in Appendix A.

The capture plant was assumed to be cooled by air with fans, some process temperatures was thus restricted by an assumed minimum cooling utility temperature which is based on an assumed ΔT_{min} , presented in Table 3.6 and the maximum ambient temperature of the season. The maximum ambient temperature during the winter and summer case was assumed to be 10 °C and 25°C, respectively.

Table 3.4: Selected design specifications for the capture processes in Aspen

	MEA	HPC	Unit
Sorbent concentration	30	30	[wt%]
Capture rate	90	90	[%]
Absorber solvent inlet temperature	40	114	[°C]
Absorber pressure	1.06	7	[bar]
Desorber pressure	1.9	1.2	[bar]
Lean loading	0.25	-	[mol/mol]
Minimum cooling utility temperature (winter)	20	20	[°C]
Minimum cooling utility temperature (summer)	35	35	[°C]

The lean loading factor for the MEA based process was selected by varying its value to find which loading factor resulted in the lowest specific reboiler duty [MW/kgCO₂]. The lean loading factor for the HPC based process was not specified as in the MEA case, but was rather a result of other specifications, such as the capture rate and sorbent concentration.

From the converged simulation of the absorption processes was power demands, heating and cooling demands and temperature intervals of the heating and cooling sources collected. The result was then used for the simulation of the integrated system in Epsilon.

3.2.3 Liquefaction simulation

The liquefaction process was also simulated with Aspen based on the work of Deng et al [31]. The process scheme in Aspen is presented in Appendix B. The liquefaction follows the capture process, the feed to the model was therefore set as the outgoing concentrated CO₂ stream from the capture plant. This stream was assumed to consist of solely CO₂, water, N₂, O₂ and MEA. The refrigerant in the refrigeration cycle was assumed to be ammonia similar to the carbon capture project at the WTE plant at Klemetsrud [43]. Further on, the specification of the outgoing CO₂ stream was set to 16 bar and -27.7 °C.

The compression train of the liquefaction process consisted of three compressor stages similar to Figure 2.7. The pressure levels of each compression stage was set to maintain a constant pressure ratio. The first compression stage thus increased the pressure to from 1.9 bar to 4.63 bar, the second to 11.28 bar. The third compression stage increased the pressure to 27.5 bar in accordance with the specifications from Deng et al. [31]. Similar to the capture simulation was the minimum cooling utility temperature in the intercoolers and pre-cooler set to 20°C and 35°C during the winter and the summer respectively.

The performance of the refrigeration cycle and liquifier was determined by assumed temperatures and pressures in the process. These conditions are in turn based on an

assumed state of the liquefied CO₂ and assumed minimum temperature differences, presented in Table 3.6. A summary of the assumed conditions are presented in Table 3.5. Furthermore, the pressure levels of the compression stages in the refrigeration cycle was determined to maintain a constant pressure ratio.

Table 3.5: Assumed parameters for liquefaction for the selected hour during winter and summer operation

	Winter	Summer	Unit
Liquifier (CO ₂ side)	-15.24, 27.5	-15.24, 27.5	[°C], [bar]
Liquifier (NH ₃ side)	-20.24, 1.4	-20.24, 1.4	[°C], [bar]
Refrigeration condenser	20.19, 9.4	35.47, 14.8	[°C], [bar]

3.3 Modelling of integration to CHP plant heat sources and heat sinks

The modelling of the heat integration between the CHP plant and CCL plant is based on the result of the modelling of the stand alone systems, where heat and cooling duties of the CO₂ capture and liquefaction process was added to the model of Renova's plant in off-design mode. The heat demand in the CCL plant was represented as a heat consumer in Epsilon and the cooling demands was represented as heat injections.

This section describes the single heat integrations between the heat demand in the reboiler and heat sources such as the hot water system, the feed water and the steam system. It also describes the single heat integrations between cooling demands in the CCL process and heat sinks in the WTE plant such as the DH system. The purpose of first simulating specific connections between the CCL plant and the CHP plant was to identify the effects of the specific change to the system. Furthermore, the power integration between the CCL process and the power sources are described in this section. A schematic picture of the integration between the CHP plant and the CO₂ capture and liquefaction plant is presented in Figure 3.3.

3. Method

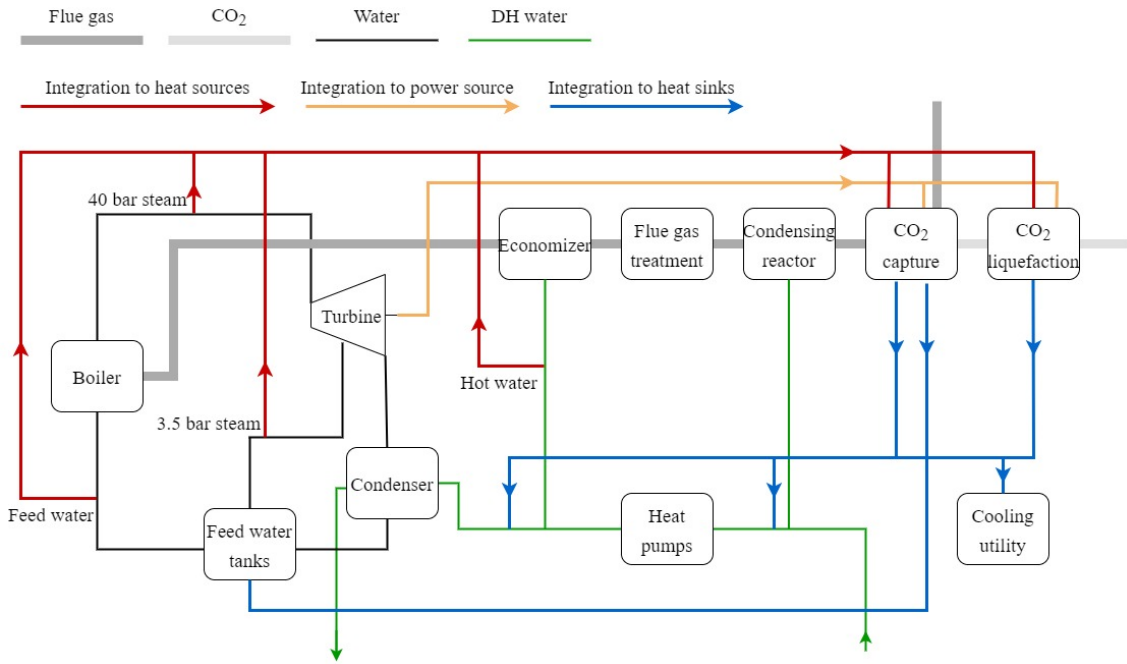


Figure 3.3: Process scheme of the Renova's CHP plant with integration to the CO₂ capture and liquefaction plant

Minimum temperature differences are assumed for heat exchange between different hot and cold fluids in the processes. The ΔT_{min} are presented in Table 3.6 and are used for all heat exchanges.

Table 3.6: Assumed minimum temperature differences

		Unit
Liquid-liquid ΔT_{min}	5	[°C]
Steam-liquid ΔT_{min}	5	[°C]
Gas-liquid ΔT_{min}	10	[°C]

3.3.1 Integration to heat sources

The integration between the heat sources in the CHP plant the the reboiler in the capture process is represented as the red line in Figure 3.3. This section will describe how heat specific heat integration to the feed water, hot water, 3.5 bar steam and 40 bar steam was performed.

In addition, for an integration between the CCL process and the feed water, the hot water system and the 3.5 bar steam, it was important to evaluate the amount of heat available from these system and how the heat could be extracted. This evaluation was performed in the Epsilon model of the CHP plant by adjusting the model design. Heat was extracted from the feed water between the feed water pumps and the boilers where the feed water temperature is the highest. The heat extraction caused a temperature decrease from the current 140°C to 130°C. More heat could

be extracted if the temperature of the feed water was decreased with 15°C instead of 10°C. However, low inlet feed water temperatures could cause damage, which is why 130°C was chosen.

For the hot water system, heat was extracted from 135°C, which is the highest temperature in the system, to 125 °C for the integration with MEA based absorption and 117°C for HPC based absorption. The temperatures were chosen based on the reboiler temperatures. The heat extracted to fulfil the heat demand in the reboiler replaced other heat demands, which otherwise would have been fulfilled by the hot water. The replaced heat demands came from a heat pump and two heat exchangers, one of which supplied heat to the DH system and the other supplied heat to the 3.5 bar steam condensate. The changes was adjusted in the Ebsilon model by decreasing the temperature of the 3.5 bar steam condensate, turning off the heat pump and turning off the heat exchanger in the DH system to the hot water system.

A process scheme of the hot water system with the intended integration is presented in Figure 3.4. The figure represent that hot water is redirected to fulfil the heat demand in the CCL plant, while the hot water stream through the heat exchangers, heat pumps and heat exchanger to the DH system is excluded.

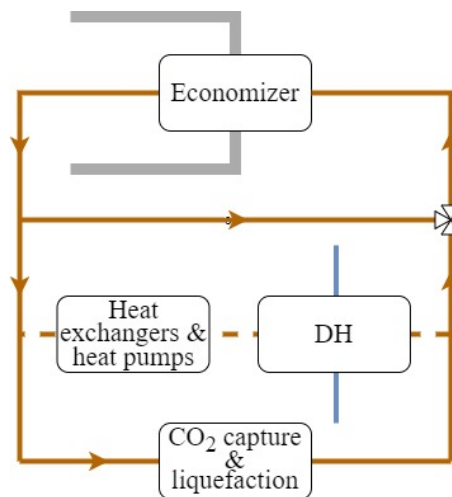


Figure 3.4: Process scheme of the hot water system with the integration to the CO₂ capture and liquefaction plant

The availability of 3.5 bar steam is limited due to a mass flow limitation of 27 kg/s in the turbine extraction. The 3.5 bar steam is utilized in other parts of the plant, eg. the absorption heat pumps and feed water regeneration. The steam available for the reboiler was therefore set as the difference between the steam currently used in the plant and the maximum possible steam extraction. The available heat from the excess 3.5 bar steam was estimated in Ebsilon by adjusting the model to extract the maximum amount of 3.5 bar possible from the turbine.

To use the 40 bar steam to heat the reboiler, two options were available: the pressure reduction station could be used to expand the steam to 3.5 bar or a new steam

turbine could be installed to expand the steam to 3.5 bar and produce electricity. The two alternatives were simulated in Epsilon with the model of the WTE plant. The pressure reduction station was simulated with a throttle which expanded the steam to 3.5 bar and a recirculation of the steam condensate to cool the superheated steam, according to Figure 3.5.

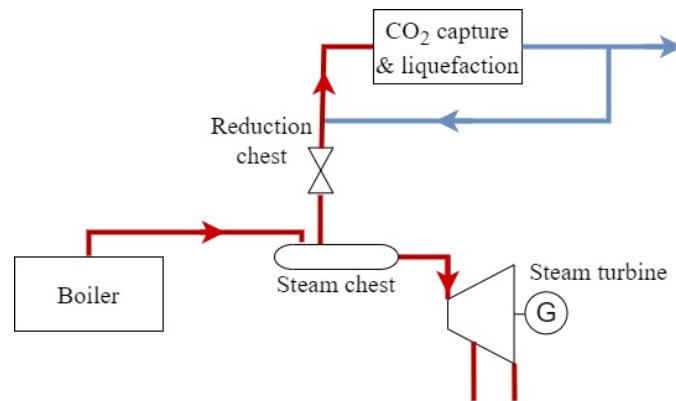


Figure 3.5: Process scheme of the pressure reduction station

The utilization of the heat from the feed water, hot water, 3.5 bar steam and 40 bar steam was prioritized based on the assumed effect on the steam cycle by extracting heat. Figure 3.6 shows the utilization prioritization for heat extraction to fulfill the heat demand in the reboiler. Based on the estimations of the available heat from the feed water, hot water and 3.5 bar steam and the utilization prioritization was different cases created to investigate which heat integration would be most preferable based on electricity and DH deliveries and cooling utilities necessary.

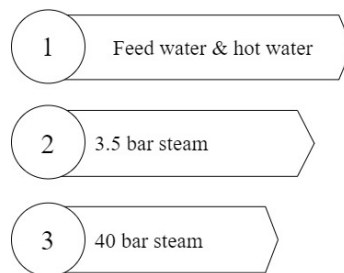


Figure 3.6: Prioritization scheme of utilization of the heat sources to fulfill the heat demand in the CO₂ capture process

3.3.2 Integration to heat sinks

The purpose of a heat integration between the CCL plant and heat sinks is to cool the CCL plant to maintain continuous operation, and to recover heat for district heating generation by extraction of heat from the condensate leaving the reboiler and from the coolers in the CO₂ capture and liquefaction process.

The temperature of the condensate leaving the reboiler depends on the design specifications in the capture process and the minimum temperature difference, according

to Table 3.6. A reboiler temperature of 120°C and a minimum temperature difference of 5°C would thus result in a condensate temperature of 125°C. The reboiler condensate is assumed to be returned to the steam cycle feed water chest, which currently operates at a temperature of 138 °C and thus has a slightly higher temperature than the reboiler condensate.

Two options are therefore possible: to return the condensate directly to the feed water chest without heat extraction for DH or to cool the condensate with DH water and then return it. The two alternatives were evaluated in Ebsilon. Figure 3.7 shows a process scheme of the district heating cycle. The heat extracted from the condensate was assumed to be injected into the DH system between the hot water system economizer and the cooling tower, as shown in Figure 3.7. The reboiler condensate was cooled to the minimum allowed temperature according the assumed minimum temperature differences in Table 3.6, i.e. the 5°C higher than the temperature of the DH water.

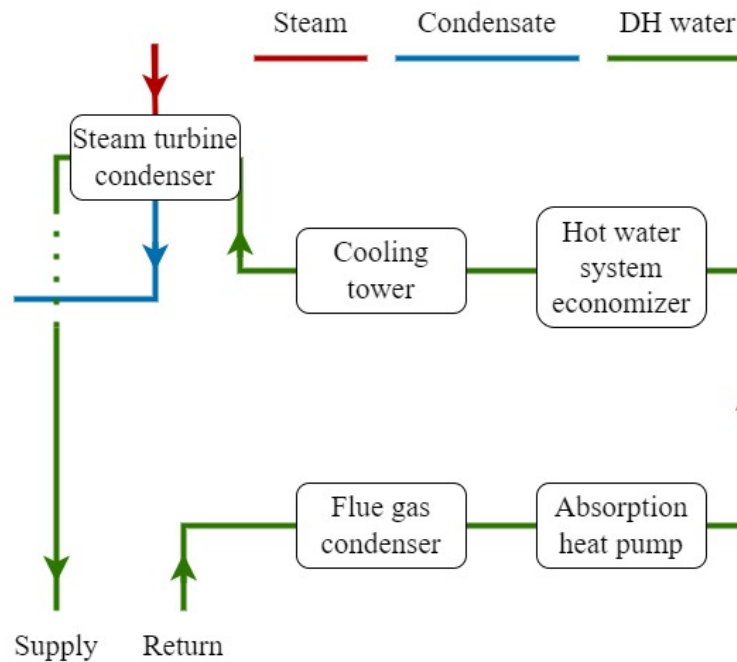


Figure 3.7: Simplified process scheme of the district heating cycle

The integration between the coolers in the CCL process and the DH system was simulated in Ebsilon and verified with a pinch analysis to ensure that the integration did not violate the assumed minimum temperature difference of 5°C.

The heat recovered from the CCL plant is integrated in the DH system by identifying locations in the DH cycle where there is a potential for increased heat injection, i.e., the DH water temperature can be increased without violating any equipment temperature restrictions. Other operational restrictions such as the minimum flow requirement of 2350 m³/h through the heat pumps were also accounted for when identifying integration locations. The temperature limitations for the existing units in the DH system depends on the temperature profile and loads of the streams

3. Method

that are cooled, which are presented in Table 3.7. These temperature and energy requirements must still be met after the integration of CCL heat sources.

Table 3.7: Stream specifications of current cooling demands fulfilled by the district heating system

	Winter			Summer		
	T_{start} [°C]	T_{target} [°C]	Load [MW]	T_{start} [°C]	T_{target} [°C]	Load [MW]
Steam	104.6	104.6	81.0	98.7	98.7	49.2
Condensing reactor	53.9	44.0	16.3	56.5	52.6	4.9
Heat pump	70.9	53.9	51.0	71.1	58.5	33.8
Economizer	128.3	108.1	6.4	127.6	108.0	4.5

The temperature profile of the DH water passing through each unit is sometimes lower than the maximum temperature allowed given a 5°C minimum temperature difference, so there is a possibility to change the temperature interval of the DH water. For a constant heat load from the existing units in the DH system, an increased cold side outlet temperature leads to a lower DH flow rate through the heat exchanger. To maintain the DH flow, a share of the original DH water must be bypassed the heat exchanger and can act as a cooling sink for the CCL plant heat integration. The gain of performing this kind of design is that the coolers in the CCL plant can be integrated with the DH water in more locations compared to if the operation of each existing unit was unchanged.

The potential for the heat transfer between the DH system and the CCL plant coolers in each integration location was determined by Ebsilon simulation and pinch analysis. A start guess of the heat transfer in all the identified locations was implemented. Due to the operation of the DH system, where the flow rate of the DH water is adjusted to fulfil all cooling demands exactly, a hot utility was not possible in the pinch analysis. If the pinch analysis concluded that a hot utility would be necessary the heat loads of the integration in the Ebsilon model were decreased by the hot utility and a new pinch analysis with new loads was performed. This method was iterated until the hot utility was 0-50kW which was assumed to be sufficiently small. Figure 3.8 show the work flow of the integration

An integration was assumed favorable if the transferred heat exceeded 1 MW, otherwise the integration would not be worth the cost of installation. This meant that coolers with a cooling demand below 1 MW was unsuitable for integration.

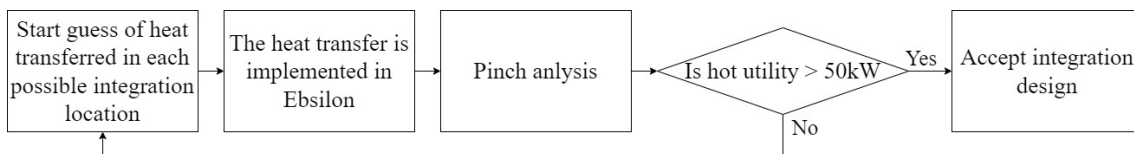


Figure 3.8: Workflow of the integration between the CCL plant and the DH system

3.3.3 Integration to power sources

The power demand in the CO₂ capture and liquefaction plant was assumed to be fulfilled by the produced electricity in the generator at the steam turbine. The power demand originates from compressors, pumps and air fans for the cooling in the CCL process. The load of the compressors and pumps was collected from the simulation of the capture and liquefaction process in Aspen.

The power demand from the air fans was calculated based on the guidance of Towler and Sinott [44]. A description of the calculations is presented in Appendix C. The power demand from the fans depends on the cooling demand from the fans which in turn depends on the level of integration to the DH system.

In addition, the internal power in the CHP plant, which was estimated to 8.3 MW during the winter and 8.2 MW during the summer, was also assumed to be constant for all simulation. However, the power demand in the CHP is expected to decrease after the integration, due to the lower volume flow through the booster fan in the flue gas treatment lines, seen in Figure 2.3. The volume flow decrease compared to the current operation since the CO₂ is removed from the stream.

3.4 Pinch analysis

This section will describe the pinch analysis used for the integration between CCL plant the coolers and the DH system. In a pinch analysis, streams with cooling demands are coupled with streams with heating demands in order to determine the amount of heat that can be exchanged internally as well as the amount of additional cooling needed to satisfy the demands. This is represented in Figure 3.9, showing a composite curve diagram. The red and blue line in the figure, also called the hot and cold composite curves, represents the cooling and heating demands distributed on a temperature-heat scale.

The total demand is thus the total length of the curve. The heat transfer between the heating and cooling demands is represented by the part of the x-axis where the curves overlap. The part of the cooling demand which does not overlap with the heating demand represents the part of the cooling demands which need cooling from an additional cold utility, which in this case is the cooling towers on the winter and air fans during the summer.

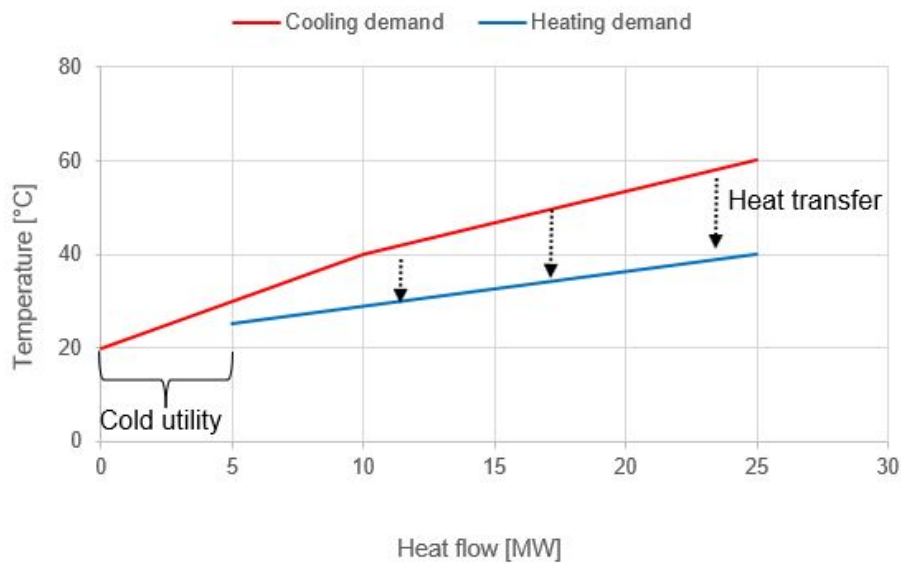


Figure 3.9: Example of a composite curve diagram

The evaluated system is presented in Figure 3.10. The evaluated system in the pinch analysis consisted of the DH system at Renova and the cooling demands which are fulfilled by the DH system such as the cooling demand in condensing reactor and economizer as well as the cooling demands in the coolers in the CO₂ capture and liquefaction process. The arrows for CO₂ capture and liquefaction, in Figure 3.10, represents the multiple coolers with different loads and temperature intervals. Which coolers that are included in the pinch analysis depends on the system and is limited since heat transfer needs to exceed 1 MW for a integration to be considered beneficial. The minimum temperature difference in the pinch analysis was assumed to be 5°C in accordance with Table 3.6.

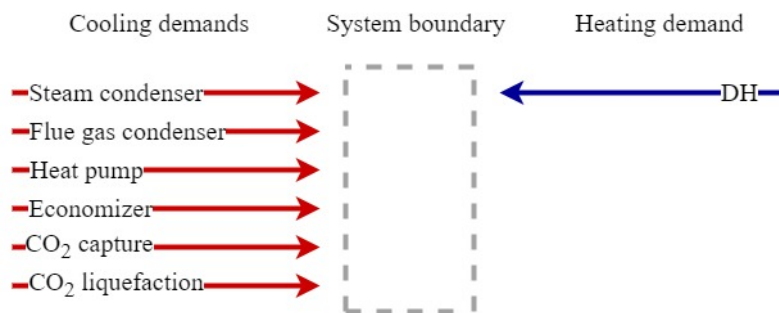


Figure 3.10: Flow sheet of the evaluated system in the pinch analysis

3.5 Case simulation

To achieve a more complete assessment of the energy performance of the integrated WTE and CCL plant, different cases were investigated. These cases described the fully integrated system including all single integration previously described. A summary of the cases is presented in Figure 3.11. The cases are divided into five areas:

capture technologies, operational point, reboiler heat source, DH temperature and heat pump capacity. The simulation of each case was performed in off-design mode in Ebsilon with modified models of Renova's CHP plant based on the integration to the CCL process.

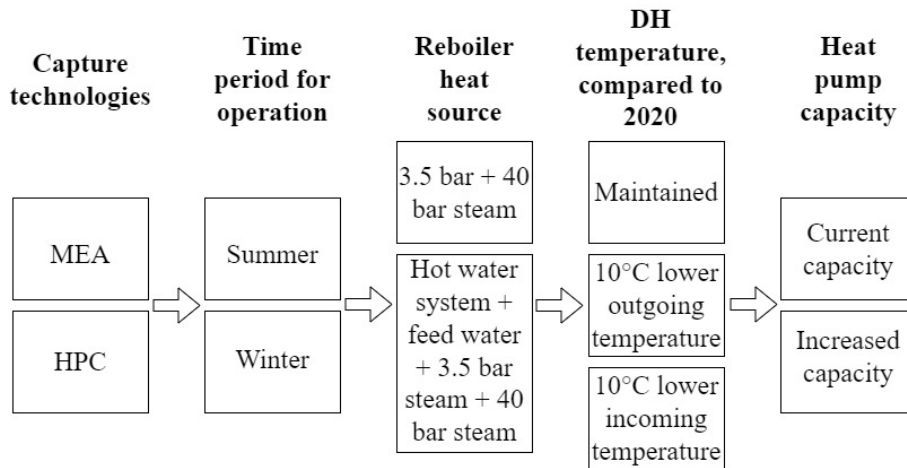


Figure 3.11: Flow sheet of the investigated cases

The cases with the different capture technologies was simulated by varying the heating, cooling and power demands of the CCL plant based on the result of each simulation in Aspen. The seasons was evaluated by adding the heating, cooling and power demands from each season to the models of Renova's CHP plant for each season.

The cases regarding reboiler heat sources is based on previous estimations of available heat in the WTE plant. The result of the estimation concluded that a limited amount of heat is available from the feed water, the hot water and 3.5 bar steam. Two cases was thus evaluated, a combination of feed water, hot water, 3.5 bar steam and 40 bar steam as heat sources and a combination 3.5 bar steam and 40 bar steam, as presented in Figure 3.11. These cases will hereafter be referred to as the *steam only case* and the *combo case*. For the first case, heat from the hot water and feed water prioritized was over heat from the 3.5 bar steam and heat 3.5 bar steam was prioritized over 40 bar steam. For the second case was 3.5 bar steam prioritized over 40 bar steam.

Three DH temperatures was investigated: a maintained temperature profile compared to Year 2020, a temperature profile with 10°C lower incoming temperature and a profile with 10°C lower outgoing temperature. The gain from lowering the outgoing DH temperature is that more heat and electricity could be produced with same amount of steam while the gain from decreasing the incoming DH temperature is that it increases the possibility of using it as cooling for the CCL process. The cases were implemented in Ebsilon by adjusting the design specification in the DH cycle to fit temperatures of each case.

Lastly, the integrated systems were investigated with two absorption heat pump capacities, the current installed capacity and a case where the capacity was increased with an additional absorption heat pump. The additional heat pump was assumed to operate similarly to the heat pumps called VP638 and VP639 currently installed. The capacity of the additional heat pump was determined with a pinch analysis where the grand composite curve of the heat pumps was added to the grand composite curve of the system described in Figure 3.10. The capacity of the absorption heat pumps was then increased until the two grand composite curves tangent, the additional capacity thus represent the capacity of the additional heat pump.

The grand composite curve of the heat pumps was constructed based on collected process data of the absorption heat pumps with the assumptions that the minimum temperature difference in the evaporator was 4°C. The result of the grand composite curves was implemented in Epsilon as a higher heat pump capacity in the DH system and a higher demand for 3.5 bar steam. The cold stream from the additional heat pump was assumed to cool the coolers in the CO₂ capture and liquefaction plant.

3.6 Energy performance evaluation

The integration between the CHP plant and the CO₂ capture and liquefaction will be evaluated based on DH and electricity supply and the additional cooling demand which require an investment. The supplied electricity from the plant, $E_{el, supplied}$ is estimated by Equation 3.1.

$$E_{el, supplied} = E_{el, produced} - E_{el, consumed} \quad (3.1)$$

The produced electricity from the turbine generator, $E_{el, produced}$ is collected from the Epsilon simulation. The consumed electricity, $E_{el, consumed}$, includes the the consumption within the CHP plant and the CCL plant. The supplied DH is estimated by Equation 3.2, since district heating is not consumed within the plant.

$$E_{DH, supplied} = E_{DH, produced} \quad (3.2)$$

The integrations will also be evaluated based on the R1 value which defines the energy efficiency of the CHP plant. The R1 value defines if a plant incinerating municipal waste should be classified as a WTE plant or a waste disposal facility according to SFS 2011:927 [45] where a WTE plant has a R1 value above 0.6. The R1 formula is defined by Equation 3.3 according to the guidelines from the European Commission [46].

$$R1 = \frac{E_{supplied} - (E_{fuel} + E_{import})}{0.97(E_{waste\ input} + E_{fuel})} \quad (3.3)$$

The supplied energy $E_{supplied}$ is defined by Equation 3.4. The energy input from fuels, E_{fuel} , the energy input from imported electricity, E_{import} and the energy input of the was, $E_{waste\ input}$, was collected from Renova's annual sustainability report [13].

$$E_{supplied} = 2.6E_{el,supplied} + 1.1E_{DH,supplied} \quad (3.4)$$

The energies in Equation 3.3 and 3.4 are given in MWh/year. Since the integration between the CHP plant and the CCL plant are evaluated for a selected hour during winter and summer operation is it thus not possible to calculate a R1-value representative for the operation of the integrated CHP plant during the whole year. Two R1-values was therefore estimated for the integrated CHP plant. The first assumes that the selected winter hour represents the operation through out the year and the second that the selected summer hour represents the operation throughout the year. The two estimated R1-values are thus considered as a minimum and maximum values for the integrated plant.

4

Results and Discussion

This chapter presents and discusses the result of the master thesis. Firstly, the result from the separate system modelling is presented, which includes the validation of the model of Renova's WTE plant and the result from the simulations of the CO₂ capture and liquefaction plant. The performance of the plants with single heat integrations between the CHP plant and CCL process is then presented and evaluated to conclude the possible arrangement for the fully integrated plants. The fully integrated plants are then presented for multiple cases regarding the capture technologies, seasons, possible heat sources for the CCL process, temperatures in the DH system and capacities for absorption heat pumps.

4.1 Modelling of stand alone processes

The following section presents and discusses the validation of Renova's CHP plant in EBSILON®Professional by comparing the simulated results with reference process data. Further on, the heating and cooling duty of the CCL plant with temperature intervals are presented from the simulation in Aspen PLUS® of the CO₂ capture and liquefaction.

4.1.1 CHP plant model validation

Table 4.1 presents the simulated electricity and DH production from the Ebsilon model of the stand alone CHP plant and reference process data. It also presents the water flow rates for selected locations in the CHP plant. Both tables presents the data for the selected hour during summer and winter operation, which is 7th of June 12 o'clock and 7th of December 12 o'clock. During the winter operation, the simulated electricity and district heating production and flow rates match the process data. During the summer operation, deviations can be seen in DH production, total DH water flow and exiting feed water flow from the feed water preheater

The produced DH deviates between the model and process data in the summer case due to the deviation of volume flow in the DH cycle. The volume flow is in Ebsilon determined by the condenser and is based on the steam input and the incoming and outgoing temperature of the DH water. The deviation in outgoing mass flow of the feed water preheater suggests that the steam input to the condenser is too small. The problem is traced back to the model setup which neglects the cooling of the 1 bar steam with feed water which will increase the mass flow of saturated steam to

the condenser. It was concluded that the deviations in DH production and some of the flows was sufficiently small to avoid a re-design of the Epsilon model of Renova's plant.

Table 4.1: Simulated electricity and district heating production and water flow rate of selected streams collected from the Epsilon model of Renova's CHP plant and from process data for the selected hour during winter and summer operation.

	Winter		Summer		
	Simulated value	Process data	Simulated value	Process data	
Produced electricity in turbine	39.15	39.72	29.86	28.73	[MW]
Produced DH in turbine condenser	189.33	191.11	123.93	127.71	[MW]
Total feed water into the boiler	74.1	74.0	56.3	56.3	[kg/s]
Total DH water	2830.4	2865.3	2066.5	2145.5	[m ³ /s]
Feed water out of the feed water preheater	52.8	53.0	37.0	38.2	[kg/s]

Figure 4.1 presents the reference steam turbine performance for two different inlet mass flows, corresponding to winter and summer operation, and a constant extraction of 3.5 bar steam. It also shows the simulated performance of the model for the same conditions. From the figure it is concluded that the model steam turbine operates similarly to the actual turbine for inlet mass flows of 67 kg/s, which corresponds to the winter case. This result thus confirms the conclusion from Table 4.1, that the model match the reference data very well for winter operation.

For a inlet mass flow of 55 kg/s, which corresponds to summer operation, the simulated turbine generates more power compared to process data. However, the power generation follows the same trend as the process data for the delivered DH temperature. It was thus concluded, based on the result from Table 4.1 and Figure 4.1, that the model of Renova's WTE plant was sufficiently accurate to describe the operation of the real plant and possible changes in operation associated with a implementation of CO₂ capture and liquefaction.

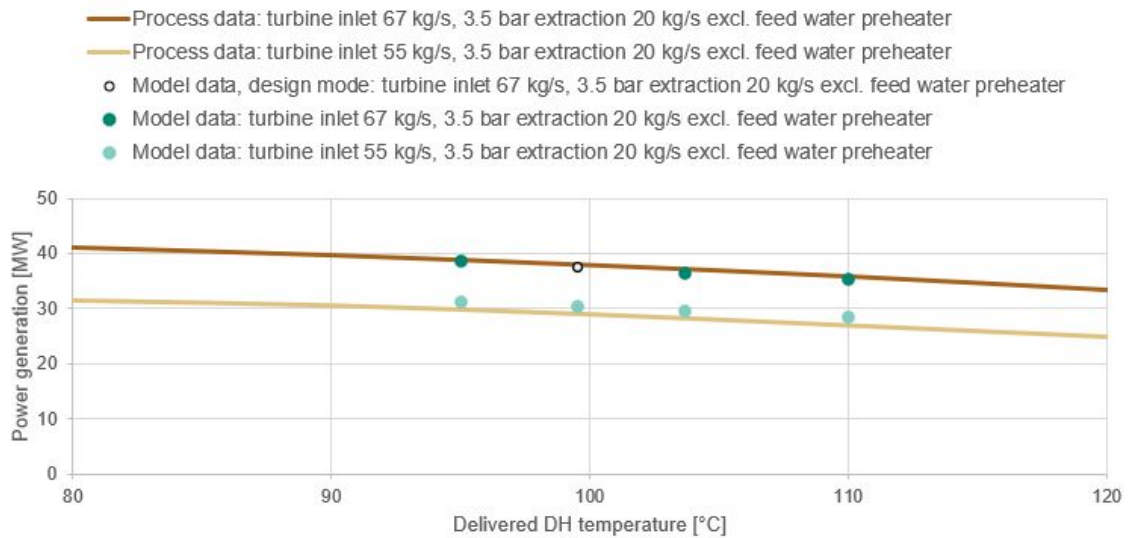


Figure 4.1: Turbine performance for different inlet mass flow collected from process data and from the Epsilon model of Renova's CHP plant. The x-axis starts from 80°C

4.1.2 Heating and cooling demands of CO₂ capture and liquefaction

The reboiler duty for the MEA and HPC based absorption, collected from the simulation in Aspen PLUS® assuming a treatment of 60% of the flue gases, is presented in Table 4.2. The table shows that the HPC based absorption has a larger heat demand compared to MEA based absorption which contradicts literature [24] and is an effect of the high demand for heat with the simulated HPC based process compared to literature. The high heat demand is a consequence of the chosen model set up and could be decreased with a lower operating temperature of the units in the CO₂ capture plant or a higher operating pressure of the absorber. Both changes would result in a higher cooling demand and for the latter alternative a higher power demand.

Table 4.2 also shows that the reboiler duty is higher for the summer operation compared to the winter operation, which is an effect of the increased temperature of the cooling utility during the summer. As mentioned, is the temperature of the cooling utility, ie. air fan, limited by the outside temperature, which results in higher cooling temperatures during the summer.

Table 4.2: Reboiler duty and temperature target of the solvent for MEA based CO₂ absorption and HPC based absorption for the selected hour during winter and summer operation

	Winter		Summer	
	T _{target} [°C]	Load [MW]	T _{target} [°C]	Load [MW]
MEA	120.1	31.3	120.1	28.9
HPC	112.0	43.2	112.0	41.0

Figure 4.2 and 4.3 shows the hot composite curves (HCC) of the cooling demands in the CO₂ capture and liquefaction process with MEA or HPC as solvent during the winter and the summer. The hot composite curves describes the distribution of the cooling demands on a temperature scale. The total cooling demand of the CCL plant is thus the maximum value for the heat flow in the hot composite curves. A description of the cooling demand of each specific cooler is presented in Appendix B.

From the graphs it can be seen that HPC has a higher maximum heat flow value compared to MEA during both the summer and the winter, which means that HPC has a higher total cooling demand compared to MEA. However, the cooling demand for HPC is more evenly distributed in temperature below 100°C compared to the MEA which has a higher cooling demand at temperatures below 45°C. This might affect the integration to the DH cycle since the available cooling the DH water can provide at lower temperatures is limited. HPC thus have a greater possibility of transferring heat from the coolers to the DH water than MEA.

The difference in appearance between MEA and HPC cooling curves arise due to the difference in origin of some of the cooling demands. HPC has a higher cooling demand of the flue gases as an effect of the compression, while MEA has a higher cooling demand in the solvent streams such as the lean solvent cooler. The different origin in cooling requirement results in diversity in distribution of cooling demands and temperature levels. Otherwise, the cooling demand in the condensers and liquefaction process are similar for MEA and HPC.

From the simulations in Aspen and the hot composite curves is it thus concluded that the cooling prerequisites for the MEA and HPC based absorption is different where HPC has a larger cooling and heating demand but may have greater possibilities for integration to the DH system while MEA has smaller cooling and heating demands but more limited possibilities for integration.

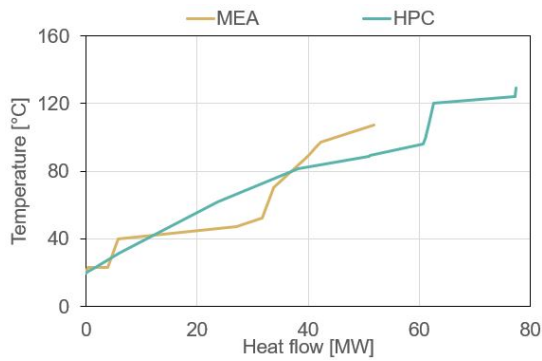


Figure 4.2: Hot composite curves of the cooling demand of the CO₂ capture and liquefaction for the selected hour during winter operation

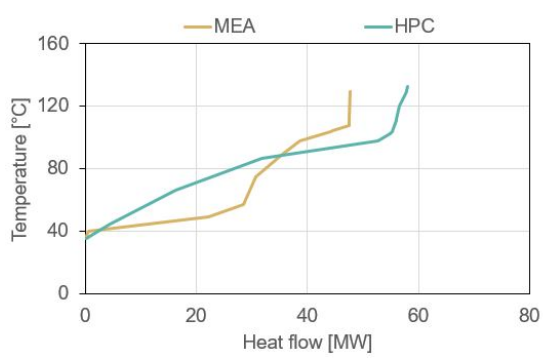


Figure 4.3: Hot composite curves of the cooling demand of the CO₂ capture and liquefaction for the selected hour during summer operation

4.2 Evaluation of integrations to CHP plant heat sources and heat sinks

This section presents the result of some of the single solutions for heat integration between the CO₂ capture and liquefaction plant and Renova's CHP plant and evaluates the preferred arrangement for the fully integrated plant. The result from the integration between the CO₂ capture and liquefaction plant and the heat sources in the CHP plant include an estimation of the available heat from the feed water, hot water and 3.5 bar steam, which are limited, and an evaluation of the solutions to utilize 40 bar steam.

The result from the integration between the CCL plant cooling demand and the heat sinks in the CHP plant focus on the possibility to recover heat from the hot condensate from the reboiler. The integration between the coolers in the CCL process focus on the possible locations in the DH system where heat can be transferred from the coolers. Lastly, a brief discussion about the impact of combining the single integration is presented.

4.2.1 Estimation of heat sources

Table 4.3 presents the share of the available heat in the feed water, hot water and 3.5 bar steam for an integration to the CCL process compared to the heat demand in the reboiler for the MEA and HPC based absorption. The results show that heat from the feed water, hot water, 3.5 bar and 40 bar steam will fulfill the demand the reboiler for the HPC based process for both summer and winter operation, while for MEA will heat from the feed water, hot water and 3.5 bar steam be sufficient to fulfill the demand. The earlier mentioned combo case will thus not include 40 bar steam for the MEA case which it will for the HPC case.

Table 4.3: Share of the estimated available heat from the feed water, the hot water, the 3.5 bar steam and the 40 bar steam compared to the reboiler demand in MEA and HPC based absorption for the selected hour during winter and summer operation

	Winter		Summer		Unit
	MEA	HPC	MEA	HPC	
Feed water	10.5	7.6	8.7	6.1	[%]
Hot water	34.7	25.2	32.2	22.6	[%]
3.5 bar steam	74.1	53.7	76.9	54.2	[%]
40 bar steam	>100	>100	>100	>100	[%]

The table also imply that the HPC based process will extract more 40 bar steam from the CHP plant compared to MEA due to the higher heat demand in the reboiler. Utilization of 40 bar steam have the greatest impact on the electricity and DH production compared to utilization of the other heat sources. This means that heat extraction for the reboiler in the HPC based absorption have a larger strain on the CHP because of the larger reboiler duty which is partly fulfilled by 40 bar steam.

4.2.2 Using 40 bar steam as a reboiler heat source

The heat integration between the reboiler and the 40 bar steam was analysed with a steam turbine and a pressure reduction station in Ebsilon. The two cases was simulated with a reboiler duty corresponding to the MEA based capture process and a heat supply consisting of 3.5 bar steam 40 bar steam, where the 3.5 bar steam was prioritized. The distribution of the produced electricity and the produced district heating out of the total electricity and DH delivery are presented in Figure 4.4 for the selected hour during winter operation of the CHP plant.

The figure shows a trade off between DH generation and electricity generation where the case with a turbine produce more relatively electricity while the case with the reduction station produce more DH. These effects arise since the reduction station requires less mass flow of the 40 bar steam to produced saturated 3.5 bar steam. This is because water is sprayed into the superheated steam after the throttle in the reduction station, according to Figure 3.5 which will saturate the steam as well as increase its mass flow. The requirement for less 40 bar steam results in a higher mass flow of steam through the current turbine and a larger heat transfer in the condenser. However, even though the original turbine produce more electricity for the reduction station case, the case with the turbine to expand the 40 bar steam will still produce more electricity in total due to the electricity production with the additional turbine.

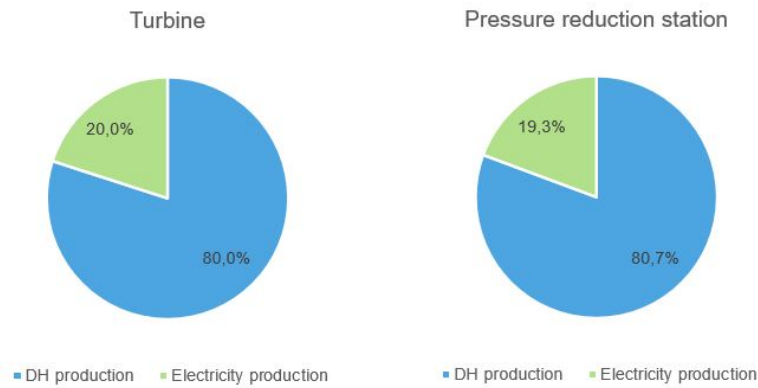


Figure 4.4: Distribution of district heating and electricity production out of the total production of DH and electricity, when 40 bar steam is expanded to 3.5 bar in a turbine or pressure reduction station. The heat demand in the reboiler corresponds to the MEA based CO₂ absorption. The figures applies to the selected hour during winter operation

The preferred arrangement for the integration between the 40 bar steam and the reboiler ultimately depends on the price electricity and DH. However, for this case was the difference in generated electricity and DH considered too small to motivate an investment of new equipment. The arrangement with the pressure reduction station was thus chosen and is implemented in all cases hereafter.

In the current case is 60% of the flue gas treated, if however 100% of the flue gas would be treated would the utilization of 40 bar steam increase since the other heat sources are limited and fully utilized which might make the turbine more advantageous compared to a pressure reduction station since the gain of electricity production would increase with the increased utilization of 40 bar steam.

4.2.3 Reboiler condensate utilization

Figure 4.5 presents the results from the simulation in Epsilon regarding the reboiler condensate, where two cases was investigated, the first when the reboiler condensate was returned to the steam cycle directly via the condensate chest, the second when the condensate was cooled to 73.6°C, transferring heat to the DH water before returning to the steam cycle. A direct return increase the electricity production with 1 MW while a DH integration favors the DH production with 1 MW. This is because the DH integration means that the condensate is returned to the steam cycle at a low temperature, lower than the steam cycle, which entail a decrease in electricity and DH production since the steam cycle will need to heat the reboiler condensate in addition to produce electricity and DH.

The preferred arrangement depends on the price of electricity and DH, similar to the cases regarding the 40 bar steam utilization. For the following simulated cases, the reboiler condensate is set to be returned directly to the steam cycle since this option results in the fewest changes on the CHP plant.

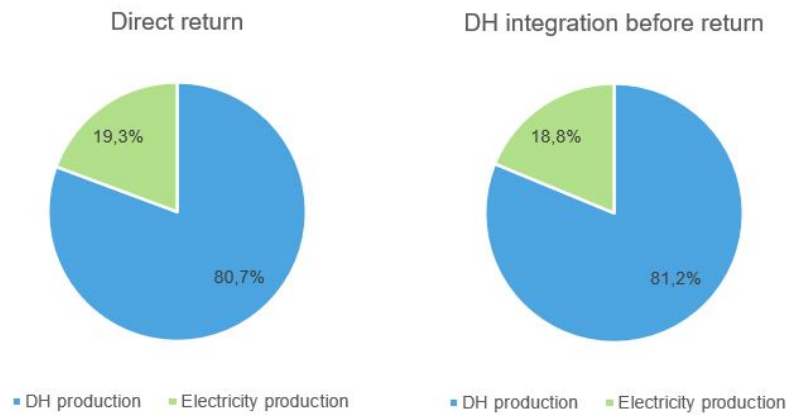


Figure 4.5: Distribution of district heating and electricity production out of the total production of DH and electricity, when the condensate from the reboiler corresponding the MEA based CO₂ based absorption is returned directly to the steam cycle and when the condensate is used to heat the district heating system and then returned to the steam cycle. The figures applies to the selected hour during winter operation

4.2.4 Integration locations in the district heating system for heat transfer from coolers

Three possible locations was identified in the district heating cycle based on the temperature and flow limitations from the heat pumps and heat exchangers which are currently installed. The three locations are demonstrated in Figure 4.6 which shows the DH cycle with the integrations locations to the CO₂ capture and liquefaction plant. "CCL integration 3" in Figure 4.6 is only possible if the temperature of the returning DH water is lower than the current levels. The outlet temperature of the integration location were set to the current temperature of the returning water.

"CCL integration 2" is possible for all cases but assumes that the heat exchanger to the condensing reactor operates in a 2 °C higher outlet temperature on the DH side compared to the current operation to enable a bypass flow to the CCL integration. "CCL integration 1" is also possible for all cases but is limited by load due to the high temperature of the water. Furthermore, a bypass on the economizer for a integration location was not necessary since CCL integration 1 was able to cover the entire possible load. A bypass on then heat pump was not possible either due to the flow limitations.

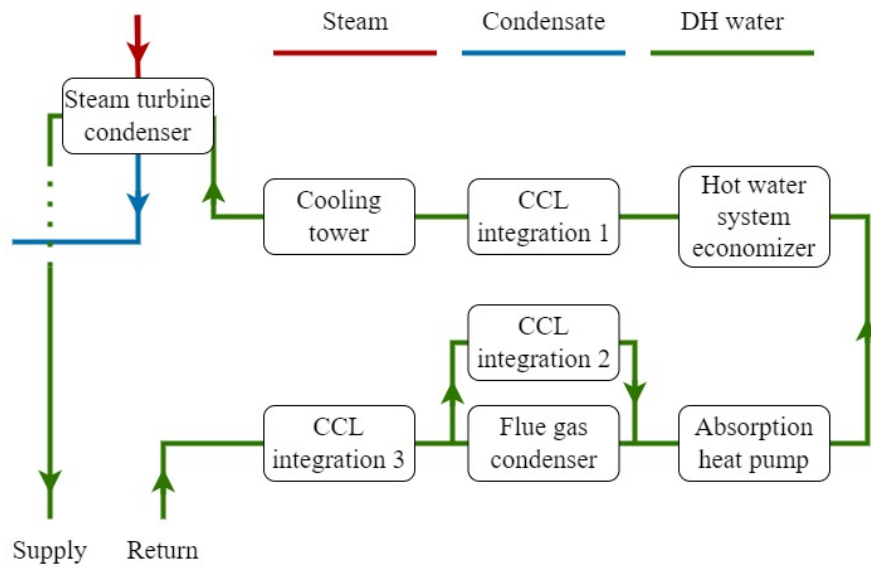


Figure 4.6: Simplified process scheme of the district heating cycle with locations for integrations to the CO₂ capture and liquefaction plant

4.2.5 Impact of combining integrations

The simulations in Epsilon of the fully integrated CHP plant showed that the integration between the heat sources in the CHP plant and the CCL plant and the integration between the heat sinks and the CCL plant complemented each other. The integration to heat sources entailed a smaller mass flow of 1 bar steam at the turbine outlet since 3.5 bar and 40 bar steam is extracted which means that the inlet flow to the turbine is smaller and that a larger flow is extracted from the 3.5 bar outlet of the turbine. As mentioned, will a smaller flow of steam at the turbine outlet result in a smaller mass flow in the DH cycle since the mass flow is determined by the condenser based on delivered heat from the steam and incoming and outgoing DH temperatures.

However, the integration to the heat sinks results in an increase in mass flow in the DH system since additional heating to the DH system means a higher temperature entering the condenser which results in a higher mass flow of DH water. Both integration arrangements is thus necessary to maintain a similar operation in the DH cycle in connection with a installation of a CO₂ capture and liquefaction plant.

4.3 Case simulation

In this section is the result from the integrated systems presented in different cases and discussed. The integrations include all previously discussed arrangement, i.e. heat integration between the heat sources and the CCL plant, the heat integration to the heat sinks and integration to the power supply.

4.3.1 Capture technologies and heat supply

Table 4.4 presents the simulated electricity and DH delivery from the CHP plant and the share DH delivery that is supplied from heat recovery from the CCL process. The table also presents the required new heat exchangers for the heat integration and the amount of utilized 40 bar steam, for the MEA and HPC based capture processes with heat supply from steam and a combination of heat sources, consisting of feed water, hot water, 3.5 bar steam and 40 bar steam. The table applies to the selected hour during winter operation. The delivered electricity is the net available electricity after the power demand in the CHP and CCL plant has been fulfilled.

Table 4.4: Simulated performance parameters of Renova’s CHP plant and the number of heat exchangers needed for the integration, when the CHP plant and CO₂ capture and liquefaction plant is fully integrated. The integration is performed for MEA and HPC with reboiler heat supply from steam only and a combination of heat sources, for the selected hour during winter operation. The reference electricity and DH delivery before the integration is also presented

	MEA		HPC		Unit
	Steam only	Combo	Steam only	Combo	
Electricity delivery	24.7	25.8	16.8	18.6	[MW]
DH delivery	187.3	186.9	203.5	201.9	[MW]
whereof DH from heat recovery	27.6	27.7	54.4	54.4	[MW]
Additional cooling demand	24.0	24.1	14.3	14.3	[MW]
40 bar steam utilization	3.19	0	7.67	2.82	[kg/s]
Required heat exchangers	12	13	14	16	
Performance before integration					
Electricity delivery			31.4		[MW]
DH delivery			189.3		[MW]

Before the integration, the modelled CHP plant delivers 31.4 MW electricity and 189.3 MW DH in the winter which means that both capture technologies cause a decrease in electricity sales of 5.6-6.7 MW for MEA and 12.8-14.6 MW for HPC. As expected, the HPC based capture process requires more power than the MEA based process due the required compression work for operation at elevated pressure levels.

Furthermore, the HPC based capture process produce 12.6-14.2 MW more DH compared the current production and the MEA based process which produce 2-2.4 MW less than current levels. This is explained by the extensive heat recovery from the CCL process to the DH system, seen in Table 4.4. The extensive heat recovery is an effect of the advantageous temperature distribution of cooling demands in the CCL process, seen in Figure 4.2, which facilitate the extensive integration of the HPC cooling demand with the DH system.

The extent of the integration is also described in Figure 4.7 and 4.8 shows the composite curves of the integrated DH system based on the system boundaries in Figure

3.10 with MEA and HPC as solvent and steam only case during winter operation. The composite curves (CC) consists of the hot and cold composite curve which describes the distribution of the cooling and heating demands in a temperature-heat diagram. The possible internal heat transfer between the cooling and heating demand are represented by the overlap between the two curves. The part of the cooling demand that does not overlap with the heating demand require additional cooling utility to be fulfilled.

Figure 4.7 and 4.8 show that the cooling and heating demand in HPC overlap over a larger area than they do for MEA. This means that more heat is transferred from the coolers in the CCL plant to the DH system in the HPC case and thus confirms the result regarding the share of the delivered DH from heat recovery in Table 3.4. The figures also show that integration with MEA is limited by the pinch point at 45°C, unlike HPC which has a pinch point at the lowest possible pinch point at 41.5°C.

The composite curves also show that the cooling towers, which represents the additional cold utility needed, will cool the system for the lowest temperatures since the DH is unable to cool the CCL process at such low temperatures.

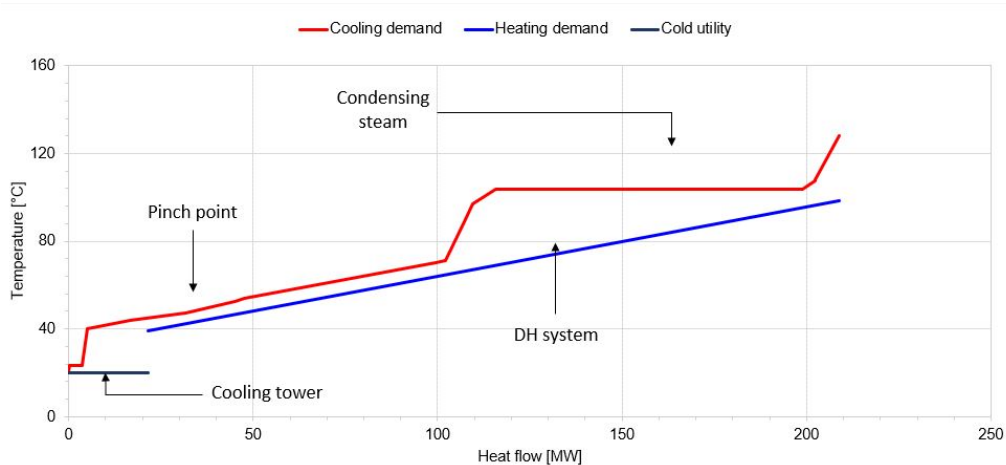


Figure 4.7: Composite curves, according to Figure 3.10, of the district heating system integrated with the CO₂ capture and liquefaction plant, utilizing MEA as solvent and with a reboiler heat supply from steam. The figure applies for the selected hour during winter operation

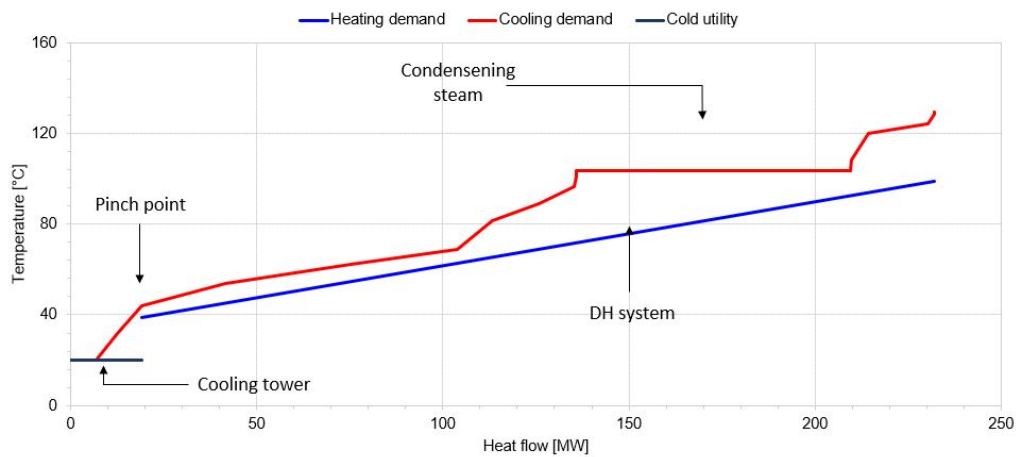


Figure 4.8: Composite curves, according to Figure 3.10, of the district heating system integrated with the CO₂ capture and liquefaction plant, utilizing HPC as solvent and with a reboiler heat supply from steam. The figure applies for the selected hour during winter operation

Table 4.4 also shows that the CCL process utilizing HPC as solvent requires more heat exchangers than MEA. This is because the process set up for HPC based absorption requires more coolers, eg. in connection with the compression of the flue gas, compared to MEA. In addition to the greater cooling demand which requires a larger investment of air fans for the summer operation, the amount of heat exchangers results in a more expensive heat integration for HPC regarding the investments costs.

The presented result concerns CO₂ treatment of 60% of the flue gases, for a CO₂ treatment of 100% of the flue gases is the energy penalty expected to increase significantly due to the increased utilization of 40 bar steam. This will be especially true for the CCL process utilizing HPC as solvent since this has a higher reboiler demand compared to MEA and already utilize more 40 bar steam, according to Table 4.4.

4.3.2 Seasonal variation

Figure 4.9 presents the deviation in electricity and DH delivery compared to the current delivery from the CHP plant without a CCL integration, when MEA and HPC is used as solvents for the capture process, for the steam only case. The figure applies for the selected hour during winter and summer operation. The winter case is relative to the current winter operation and the summer case is relative to the current summer operation. Current summer operation delivers 21.7 MW electricity and 123.9 MW DH.

The delivery of district heating during the summer can not exceed the current levels due to low demand for DH. If more heat would be supplied to the DH system would thus additional cooling capacity be needed to maintain the current DH delivery.

This limits the integration between the coolers in the CCL plant and the DH system for the HPC case during the summer, which without constraints could produce more district heating. Since the MEA case never produce more DH compared to the current production will this limitation not impact this case.

Figure 4.9 shows that the deviation in DH delivery increase for the summer case compared to the winter case for both MEA and HPC. This is an effect of the higher temperatures in the DH cycle during the summer which limits the heat recovery from the coolers in the CCL process. Cooling at lower temperatures, such as 40-50 °C, is thus not possible during the summer case. The figure also shows a small change in electricity delivery compared to the reference cases for the winter and summer case, where the summer case deviate less in electricity delivery compared to the reference case than the winter case does.

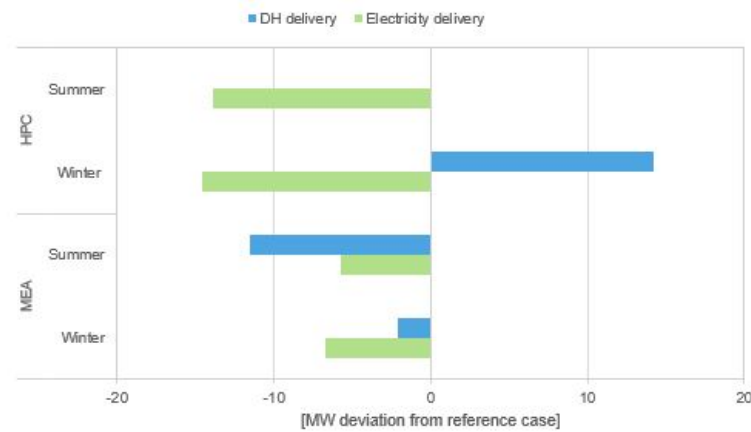


Figure 4.9: Deviation in electricity and DH delivery compared to the delivery from Renova's CHP plant without the integration, when the CHP plant is integrated with the CO₂ capture and liquefaction plant with MEA and HPC based absorption and with a reboiler heat supply from steam. The figure applies for the selected hour during winter and summer operation

Table 4.5 presents the additional cooling utility investment of air fans for the CCL process. This investment is not necessary during the winter since the existing cooling systems, such as the cooling towers, are available to meet the cooling demand. The additional cooling demand during the summer is comparably high relative to the additional cooling demand during the winter, presented in Table 4.4. The higher cooling demand arise due to the higher temperatures in the DH system which limits the integration between the coolers in the CCL plant and the DH system. As a result, the new cooling utility investment for cooling increase.

Table 4.5: New cooling investment required for the CO₂ capture and liquefaction plant, when the CHP plant is integrated with the capture and liquefaction plant with MEA and HPC based absorption and with a reboiler heat supply from steam. The table applies for the selected hour during summer operation

	MEA	HPC	Unit
New cooling investment	28.3	23.2	[MW]

By limiting the operation of the CO₂ capture and liquefaction plant to the avoid summer operation is thus extensive investments in cooling systems avoided. However, seasonal operation also results in a reduction of the total capture of CO₂ throughout the year. In addition, seasonal operation results in a higher specific cost per collected CO₂ compared to maintained operation throughout the year, since the total capture of carbon dioxide will decrease with seasonal operation. For more conclusive results is an economical evaluation regarding the operational costs and the investments costs of the CCL process is required.

4.3.3 Impact of DH return and supply temperature

The impact of altering the return and supply temperatures in the DH system is presented in Figure 4.10. The figure shows the deviation in electricity and DH delivery compared to the current delivery during winter operation for the steam only case.

The figure confirms that a lower returning DH temperature will increase the DH production since the possibility for heat integration between the coolers in the CCL process and the DH system increase. It also shows that the impact of lowering the return temperature is greater for MEA, which increase with 16.3 MW relative to the case with a maintained DH temperature profile, compared to HPC, which increase with 4.2 MW relative to the case with a maintained DH temperature profile. This is an effect of the distribution of the cooling demands in the CCL plant on the temperature scale, shown by the hot composite curves in Figure 4.2 and 4.3, where MEA has a higher distribution of cooling demand at lower temperatures compared to HPC and will thus benefit from a lower return temperature.

Figure 4.10 also confirms that a lower DH supply temperature will increase the electricity delivery since the steam at the turbine outlet will be expanded further than 1 bar. This effect cause an equally large increase in electricity delivery between MEA and HPC

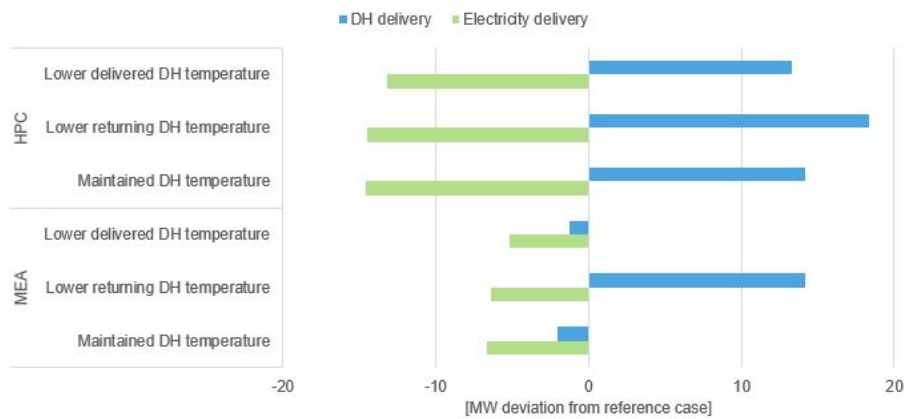


Figure 4.10: Deviation in electricity and DH delivery compared to the delivery from Renova’s CHP plant without the integration, when the CHP plant is integrated with the CO₂ capture and liquefaction plant with MEA and HPC based absorption and with a reboiler heat supply from steam, for different DH temperatures. The figure applies to the selected hour during winter operation

4.3.4 Impact of increased heat pump capacity

This part presents the results from the analysis regarding the heat pump capacity, which evaluated the effects of adding a new absorption heat pump to the DH system in addition to the current installed capacity. The grand composite curves of the system described in Figure 3.10 and the system for the absorption heat pumps with and without the additional heat pump, is presented in Figure 4.11. The figure represents the case when the CHP plant is integrated with the CCL plant with MEA as solvent and a reboiler heat supply from steam for winter operation.

Figure 4.11 shows the difference in heating capacity between the current and new heat pump systems. It also shows that the new capacity tangent with the integrated DH system, which means that the heat pump system is maximized in heating capacity. This can be compared to the graph for the current heat pump system which does not tangent with the DH system and is therefore not maximized in capacity for the integrated DH system. The additional demand for 3.5 bar steams in the new absorption heat pump and the additional available cooling water from the new heat pump is also represented in the figure.

The pinch analysis concluded that an absorption heat pump of 7.6 MW heating capacity could be added to the DH system when MEA is utilized as solvent in the absorption and 15.2 MW heating capacity for HPC.

4. Results and Discussion

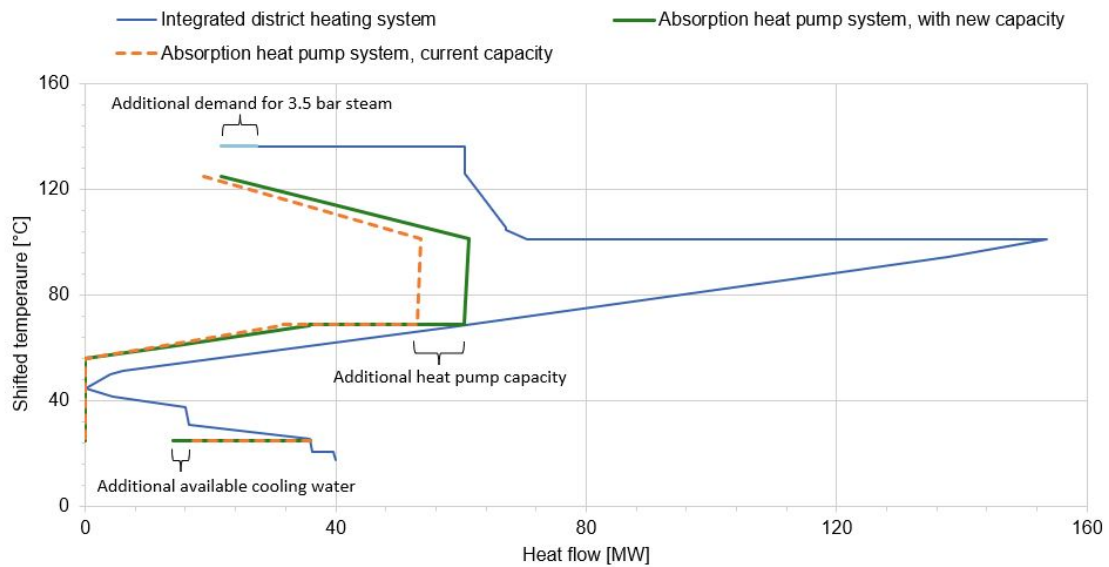


Figure 4.11: Grand composite curves of the district heating system and the absorption heat pumps with an additional heat pump compared to the current operated capacity, when the CHP plant is integrated with the CO₂ capture and liquefaction plant with MEA based absorption and with a reboiler heat supply from steam. The figure applies to the selected hour during winter operation

Figure 4.12 shows the result from the simulations in the Epsilon model of the integrated systems with an additional absorption heat pump and with the current heat pump capacity. The simulation was performed with a heat supply for the CCL plant from steam during winter operation. The figures show a gain of delivered DH and a loss of delivered electricity from installing an additional absorption heat pump to the DH system.

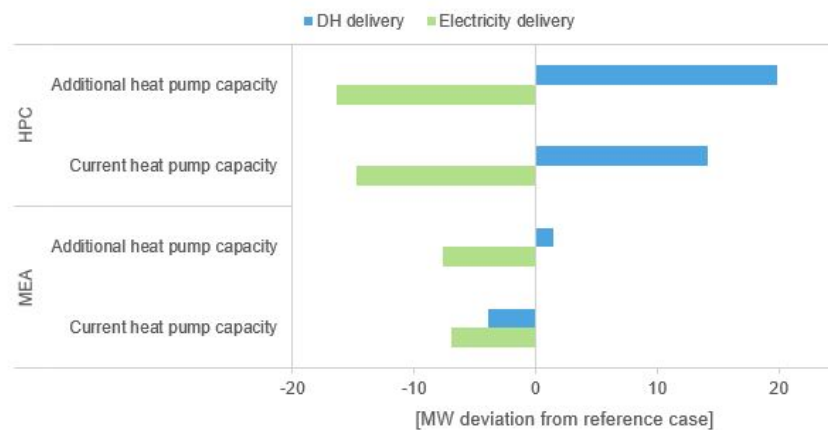


Figure 4.12: Deviation in electricity and DH delivery compared to the delivery from Renova's CHP plant without the integration, when the CHP plant is integrated with the CO₂ capture and liquefaction plant with MEA and HPC based absorption and with a reboiler heat supply from steam, for different absorption heat pumps capacities. The figure applies to the selected hour during winter operation

4.4 Summarizing evaluation

A summary of the result from the case simulations is presented in Figure 4.13 which represents the electricity and DH delivery from each case during winter operation. Based on the figure with reference to result from Table 4.4, Figure 4.10 and 4.12 will an integration between Renova's CHP plant and a CO₂ capture and liquefaction with HPC based absorption, a reboiler heat supply from 3.5 bar steam and 40 bar steam and an additional absorption heat pump with a heating capacity of 15.2 MW during winter operation result in the highest delivery of district heating of 209.2 MW with 15.0 MW delivered electricity. This corresponds to a gain of the total delivered electricity and DH of 1.5% compared to the current delivery for the selected hour during winter operation.

An integration with the MEA based absorption, a reboiler heat supply from hot water, feed water and 3.5 bar steam and a 10 °C lower delivered DH temperature during winter operation results in the highest delivery of electricity of 27.7 MW with 187 MW DH. This corresponds to a loss of the total delivered electricity and DH of 2.7% compared to the current delivery for the selected hour during winter operation. This arrangement also achieves an electricity and DH delivery most similar to the current delivery without a implementation of a CCL plant

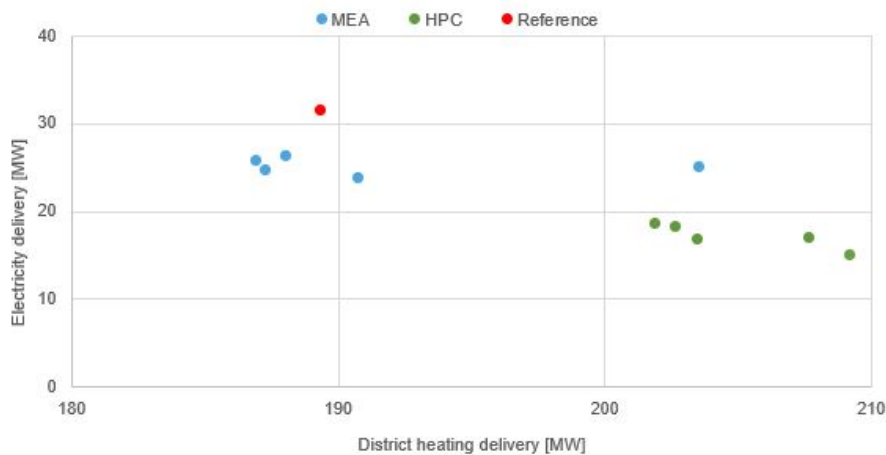


Figure 4.13: Summary of the result from the case simulation, represented in electricity and district heating delivery. The reference refers to the delivery from the current CHP plant. The figure applies to the selected hour during winter operation

Table 4.6 presents the R1-values and energy deliveries, i.e. the total delivery of electricity and DH, for Renova's WTE CHP plant when the CHP plant is integrated with the CO₂ capture and liquefaction plant with MEA and HPC based absorption and with a reboiler heat supply from steam or a combination of heat sources. The table applies to the selected hour during summer and winter operation. The reference case corresponds to the performance of the CHP plant without an integration to the CCL plant. The R1-value exceeds 0.6, which entail that Renova's plant in Sävenäs will continue to be classified as a WTE plant rather than an waste disposal facility.

Table 4.6: Energy performance of Renova’s CHP plant when the CHP plant is integrated with the CO₂ capture and liquefaction plant with MEA and HPC based absorption and with a reboiler heat supply from steam and a combination of heat sources. The reference corresponds to the performance of the CHP without the integration. The reference case The table applies to the selected hour during summer and winter operation

	Reference	MEA		HPC	
		Steam only	Combo	Steam only	Combo
Winter					
R1-value	1.31	1.48	1.50	1.47	1.48
Energy delivery	1.00	0.96	0.96	0.99	0.99
Summer					
R1-value	1.31	0.91	0.92	0.86	0.88
Energy delivery	1.00	0.58	0.59	0.60	0.60

The table also shows that the highest energy delivery is achieved with HPC as solvent for the CO₂ capture, both during winter and summer operation, which is an effect of the extensive heat recovery from the CCL plant which benefits the DH production. However, the preferred arrangement for integration between the CHP plant and the CCL plant will depend on the price of electricity and district heating in the future which will determine if a high energy delivery with high DH delivery is advantageous or if a lower energy delivery with high electricity delivery is preferred.

5

Conclusion

In this thesis, the integrations between a CO₂ capture and liquefaction plant and Renova's combined heat and power (CHP) plant have been evaluated with respect to the operational constraints of the CHP plant. The integration was evaluated for two different CO₂ absorption technologies utilizing monoethanolamine (MEA) or hot potassium carbonate (HPC). The results show that the integrations which recover heat from the CO₂ capture and liquefaction plant to the CHP plant entails a significant gain in district heating delivery, where 28-64 MW heat can be recovered depending on solvent.

The MEA based absorption results in a greater loss in district heating delivery than the HPC based, where ~99% of the district heating delivery is retained. The HPC based process with heat recovery results a 7% increase in district heating supply relative to current levels. However, the HPC based absorption also results in a considerable loss in electricity delivery - ~56% retained electricity delivery, which could be compared to ~80% with MEA.

The case simulations, where the integrated CHP and CO₂ capture and liquefaction plant were varied with different capture technologies, reboiler heat supplies, district heating temperature profiles and absorption heat pump capacities, resulted in an electricity delivery of 48-88% of the retained electricity delivery. The maximum value is achieved with MEA as CO₂ absorber, a capture process heat supply from a combination of heat sources such as feed water and a lower returning district heating water temperature. The case simulation also resulted in a district heating delivery of 99-116% of the current delivery, where the maximum value is achieved with HPC, a capture process heat supply from steam and an additional heat pump of 15.5 MW heat capacity.

Furthermore, the integration between the plants was investigated for winter and summer operation. It was found that operation is preferred during the winter, due to the required additional cooling investment of 28.3 MW for MEA and 23.2 MW for HPC during the summer. From this aspect would it thus be advantageous to operate the CO₂ capture and liquefaction plant solely during the winter. In addition, the higher cost in cooling equipment in combination with the need for more heat exchangers with compared to MEA results in a higher investment cost for the integration. Therefore, it is recommended to perform an economic analysis of the option to solely operate the CCS plant during the winter season.

5. Conclusion

Finally, this project concludes that heat integrations between a CHP plant and CO₂ capture and liquefaction plant have large impacts on the district heating and electricity delivery and that significant gains can be achieved by heat recovery. The project also concludes that the arrangements for the heat integration are important, and the chosen arrangement will depend on the value of heat and power.

Bibliography

- [1] J. Delbeke, A. Runge-Metzger, Y. Slingenber, and J. Werksman, “The paris agreement,” *Towards a Climate-Neutral Europe: Curbing the Trend*, pp. 24–45, 2019. DOI: 10.4324/9789276082569-2. [Online]. Available: https://unfccc.int/sites/default/files/english_paris_agreement.pdf.
- [2] Ministry of the environment and Government offices of Sweden, “Sweden’s long-term strategy for reducing greenhouse gas emissions,” *Unfccc*, no. December, 2020. [Online]. Available: https://unfccc.int/sites/default/files/resource/LTS1_Sweden.pdf.
- [3] Working Group III of the Intergovernmental Panel on Climate, “IPCC Special Report on Carbon Dioxide Capture and Storage,” Cambridge University, Cambridge, New York, Tech. Rep., 2005, p. 442. [Online]. Available: https://www.ipcc.ch/site/assets/uploads/2018/03/srccs_wholereport-1.pdf.
- [4] “Introduction to Industrial Carbon Capture and Storage,” *Global Carbon Capture and Storage Institute*, p. 4, 2016.
- [5] D. T. Kearns, “Waste-to-Energy with CCS: A pathway to carbon-negative power generation,” *Global CCS Institute*, pp. 1–11, 2018. [Online]. Available: https://www.globalccsinstitute.com/wp-content/uploads/2019/10/Waste-to-Energy-Perspective_October-2019-5.pdf.
- [6] 2050 Consulting, “Hur når Sverige fossilfri energiåtervinning från avfallsförbränning?” *Avfall Sverige*, p. 38, 2021.
- [7] J. Sahlin, M. Solis, M. Bisailion, M. Edo, C. Jensen, and I. Johansson, “Bränslekalitet - Nuläge och scenarier för sammansättningen av restavfall till år 2025,” *Avfall Sverige*, Malmö, Tech. Rep., 2019, p. 138.
- [8] J. Andersson, “An investigation of carbon capture technologies for Sävenäs waste-to-energy plant,” Luleå University of Technology, Tech. Rep., 2020.
- [9] Stockholm Exergi, *Bio-CCS*. [Online]. Available: <https://www.stockholmexergi.se/minusutslapp/beccs/>.
- [10] N. V. Khartchenko and V. M. Kharchenko, *Advanced Energy Systems*. Boca Roca, UNITED STATES: CRC Press LLC, 2013, pp. 205–206, ISBN: 9781482216882. [Online]. Available: <http://ebookcentral.proquest.com/lib/chalmers/detail.action?docID=1466928>.
- [11] K. Darrow, R. Tidball, J. Wang, and A. Hampson, “Catalog of CHP Technologies,” U.S. Environmental Protection Agency Combined Heat and Power Partnership, Tech. Rep. September, 2017. [Online]. Available: https://www.epa.gov/sites/default/files/2015-07/documents/catalog_of_chp_technologies.pdf.

- [12] Renova, “Från avfall till ren energi,” Tech. Rep., 2014, p. 16. [Online]. Available: https://www.renova.se/globalassets/fran_avfall_till_ren_energi.pdf.
- [13] “Hållbarhetsredovisning: 2020,” Renova, Tech. Rep., 2020. [Online]. Available: https://www.renova.se/globalassets/renova/om-renova/renova_hallbarhetsredovisning_2020_tillg.pdf.
- [14] J. Gibbins and H. Chalmers, “Carbon capture and storage,” *Energy Policy*, vol. 36, no. 12, pp. 4317–4322, 2008, ISSN: 0301-4215. DOI: <https://doi.org/10.1016/j.enpol.2008.09.058>. [Online]. Available: <https://www.sciencedirect.com/science/article/pii/S0301421508004436>.
- [15] J. Wilcox, *Introduction to Carbon Capture*. 2012, pp. 1–34, ISBN: 9781461422143. DOI: [10.1007/978-1-4614-2215-0](https://doi.org/10.1007/978-1-4614-2215-0){_}1.
- [16] M. Bui, C. S. Adjiman, A. Bardow, E. J. Anthony, A. Boston, S. Brown, P. S. Fennell, S. Fuss, A. Galindo, L. A. Hackett, J. P. Hallett, H. J. Herzog, G. Jackson, J. Kemper, S. Krevor, G. C. Maitland, M. Matuszewski, I. S. Metcalfe, C. Petit, G. Puxty, J. Reimer, D. M. Reiner, E. S. Rubin, S. A. Scott, N. Shah, B. Smit, J. P. Trusler, P. Webley, J. Wilcox, and N. Mac Dowell, “Carbon capture and storage (CCS): The way forward,” *Energy and Environmental Science*, vol. 11, no. 5, pp. 1062–1176, 2018, ISSN: 17545706. DOI: [10.1039/c7ee02342a](https://doi.org/10.1039/c7ee02342a).
- [17] D. Bjørnsen, J. Kjærstad, D. Langlet, A. Mathisen, P. Aagaard, and A. Anundskås, “Carbon Capture and Storage in the Skagerrak/Kattegat region,” Chalmers University University of Oslo Göteborgs University Tel-tek, Tech. Rep., 2012. [Online]. Available: <http://interreg-oks.eu/webdav/files/gamla-projektbanken/se/Material/Files/Kattegat/Skagerrak/Dokumenter+projektbank/CCS%20final%20report.pdf>.
- [18] Y. Wang, L. Zhao, A. Otto, M. Robinius, and D. Stolten, “A Review of Post-combustion CO₂ Capture Technologies from Coal-fired Power Plants,” *Energy Procedia*, vol. 114, no. November 2016, pp. 650–665, 2017, ISSN: 18766102. DOI: [10.1016/j.egypro.2017.03.1209](https://doi.org/10.1016/j.egypro.2017.03.1209). [Online]. Available: <http://dx.doi.org/10.1016/j.egypro.2017.03.1209>.
- [19] K. Li, A. Cousins, H. Yu, P. Feron, M. Tade, W. Luo, and J. Chen, “Systematic study of aqueous monoethanolamine-based CO₂ capture process: Model development and process improvement,” *Energy Science and Engineering*, vol. 4, no. 1, pp. 23–39, 2016, ISSN: 20500505. DOI: [10.1002/ese3.101](https://doi.org/10.1002/ese3.101).
- [20] N. Pour, P. A. Webley, and P. J. Cook, “Potential for using municipal solid waste as a resource for bioenergy with carbon capture and storage (BECCS),” *International Journal of Greenhouse Gas Control*, vol. 68, no. February 2017, pp. 1–15, 2018, ISSN: 17505836. DOI: [10.1016/j.ijggc.2017.11.007](https://doi.org/10.1016/j.ijggc.2017.11.007). [Online]. Available: <https://doi.org/10.1016/j.ijggc.2017.11.007>.
- [21] R. Notz, H. P. Mangalapally, and H. Hasse, “Post combustion CO₂ capture by reactive absorption: Pilot plant description and results of systematic studies with MEA,” *International Journal of Greenhouse Gas Control*, vol. 6, pp. 84–112, 2012, ISSN: 17505836. DOI: [10.1016/j.ijggc.2011.11.004](https://doi.org/10.1016/j.ijggc.2011.11.004). [Online]. Available: <http://dx.doi.org/10.1016/j.ijggc.2011.11.004>.

- [22] X. Luo and M. Wang, “Optimal operation of MEA-based post-combustion carbon capture for natural gas combined cycle power plants under different market conditions,” *International Journal of Greenhouse Gas Control*, vol. 48, pp. 312–320, 2016, ISSN: 1750-5836. DOI: <https://doi.org/10.1016/j.ijggc.2015.11.014>. [Online]. Available: <https://www.sciencedirect.com/science/article/pii/S1750583615301304>.
- [23] K. H. Smith, N. J. Nicholas, and G. W. Stevens, *Inorganic salt solutions for post-combustion capture*, x. Elsevier Ltd, 2016, pp. 145–166, ISBN: 9780081005156. DOI: 10.1016/B978-0-08-100514-9.00007-X. [Online]. Available: <http://dx.doi.org/10.1016/B978-0-08-100514-9.00007-X>.
- [24] S. Bergström, “Koldioxidavskiljning på ett biobränsleeldat kraftvärmeverk - Simulering av två avskiljningstekniker vid Karlstad Energis kraftvärmeverk, Heden 3,” Karlstad Universitet, Tech. Rep., 2020.
- [25] K. Gustafsson, R. Sadegh-Vaziri, S. Grönkvist, F. Levihn, and C. Sundberg, “BECCS with combined heat and power: Assessing the energy penalty,” *International Journal of Greenhouse Gas Control*, vol. 108, no. April, 2021, ISSN: 17505836. DOI: 10.1016/j.ijggc.2020.103248.
- [26] F. K. Ayittey, C. A. Obek, A. Saptoro, K. Perumal, and M. K. Wong, “Process modifications for a hot potassium carbonate-based CO₂ capture system: a comparative study,” *Greenhouse Gases: Science and Technology*, vol. 10, no. 1, pp. 130–146, 2020, ISSN: 21523878. DOI: 10.1002/ghg.1953.
- [27] Å. Eliasson and E. Fahrman, “Utilization of Industrial Excess Heat for CO₂ Capture Effects on Capture Process Design and District Heating Supply,” Chalmers University of Technology, Tech. Rep., 2020.
- [28] COWI, “CinfraCap-Gemensam infrastruktur för transport av koldioxid,” 2021. [Online]. Available: <https://www.goteborgshamn.se/globalassets/cinfracap-forstudie-23-april-2021.pdf>.
- [29] EQUINOR, *Northern Lights FEED report*.
- [30] U. Zahid, J. An, U. Lee, S. P. Choi, and C. Han, “Techno-economic assessment of CO₂ liquefaction for ship transportation,” *Greenhouse Gases: Science and Technology*, 2014. DOI: ghg.
- [31] H. Deng, S. Roussanaly, and G. Skaugen, “Techno-economic analyses of CO₂ liquefaction: Impact of product pressure and impurities,” *International Journal of Refrigeration*, vol. 103, pp. 301–315, 2019, ISSN: 01407007. DOI: 10.1016/j.ijrefrig.2019.04.011.
- [32] STEAG, “EBSILON®Professional: The Planning Tool for the Power Plant Process,” Zwingenberg, Germany, Tech. Rep.
- [33] aspentech, *Aspen Plus®*. [Online]. Available: <https://mc-8041da91-139d-4acf-82e4-8766-cd.azurewebsites.net/en/products/engineering/aspens-plus>.
- [34] S. Ó. Gardarsdóttir, F. Normann, K. Andersson, and F. Johnsson, “Postcombustion CO₂ Capture Using Monoethanolamine and Ammonia Solvents: The Influence of CO₂ Concentration on Technical Performance,” *Industrial & Engineering Chemistry Research*, vol. 54, no. 2, pp. 681–690, Jan. 2015, ISSN: 0888-5885. DOI: 10.1021/ie503852m. [Online]. Available: <https://pubs.acs.org/doi/10.1021/ie503852m>.

- [35] M. Biermann, F. Normann, F. Johnsson, and R. Skagestad, "Partial Carbon Capture by Absorption Cycle for Reduced Specific Capture Cost," *Industrial & Engineering Chemistry Research*, vol. 57, no. 45, acs.iecr.8b02074, Oct. 2018, ISSN: 0888-5885. DOI: 10.1021/acs.iecr.8b02074. [Online]. Available: <https://pubs.acs.org/doi/10.1021/acs.iecr.8b02074>.
- [36] A. S. Berrouk and R. Ochieng, "Improved performance of the natural-gas-sweetening Benfield-HiPure process using process simulation," *Fuel Processing Technology*, vol. 127, pp. 20–25, 2014, ISSN: 0378-3820. DOI: <https://doi.org/10.1016/j.fuproc.2014.06.012>. [Online]. Available: <https://www.sciencedirect.com/science/article/pii/S0378382014002495>.
- [37] T. N. G. Borhani, V. Akbari, M. K. A. Hamid, and Z. A. Manan, "Rate-based simulation and comparison of various promoters for CO₂ capture in industrial DEA-promoted potassium carbonate absorption unit," *Journal of Industrial and Engineering Chemistry*, vol. 22, pp. 306–316, 2015, ISSN: 22345957. DOI: 10.1016/j.jiec.2014.07.024.
- [38] K. A. Mumford, K. H. Smith, C. J. Anderson, S. Shen, W. Tao, Y. A. Suryaputradinata, D. M. Quyn, A. Qader, B. Hooper, R. A. Innocenzi, S. E. Kentish, and G. W. Stevens, "Post-combustion capture of CO₂: Results from the Solvent absorption capture plant at hazelwood power station using potassium carbonate solvent," *Energy and Fuels*, vol. 26, 2012, ISSN: 08870624. DOI: 10.1021/ef3015519.
- [39] N. P. Devries, "CO₂ Absorption into Concentrated Carbonate Solutions with Promoters at Elevated Temperatures," University of Illinois at Urbana-Champaign, Tech. Rep., 2014.
- [40] G. T. Rochelle, E. Chen, B. Oyenekan, A. Sexton, J. Davis, M. Hilliard, and A. Veawab, "CO₂ Capture by Absorption with Potassium Carbonate, Second Quarterly Progress Report," Department of Chemical Engineering The University of Texas at Austin, Tech. Rep., 2006.
- [41] S. Zhou, S. Wang, C. Sun, and C. Chen, "SO₂ effect on degradation of MEA and some other amines," *Energy Procedia*, vol. 37, pp. 896–904, 2013, ISSN: 1876-6102. DOI: <https://doi.org/10.1016/j.egypro.2013.05.184>. [Online]. Available: <https://www.sciencedirect.com/science/article/pii/S187661021300194X>.
- [42] I. Ustadi, T. Mezher, and M. R. Abu-Zahra, "Potential for Hybrid-Cooling System for the CO₂ Post-Combustion Capture Technology," *Energy Procedia*, vol. 114, no. November 2016, 2017, ISSN: 18766102. DOI: 10.1016/j.egypro.2017.03.1771.
- [43] Fortum Oslo Varme, "Project CCS: Carbon Capture Oslo: Klemetsrubanlegget," Tech. Rep., 2018. [Online]. Available: https://ccsnorway.com/wp-content/uploads/sites/6/2019/09/fortum_oslo_varme.pdf.
- [44] G. Towler and R. Sinnott, *Chemical Engineering Design : Principles, Practice and Economics of Plant and Process Design*. Elsevier Science & Technology, 2012.
- [45] *Avfallsförordning (2011:927)*, 2011. [Online]. Available: https://www.riksdagen.se/sv/dokument-lagar/dokument/svensk-forfattningssamling/avfallsforordning-2011927_sfs-2011-927.

- [46] European Commission, “Guidelines on the R1 energy efficiency formula in Annex II of Directive,” 2008. [Online]. Available: <https://ec.europa.eu/environment/pdf/waste/framework/guidance.pdf>.

A

Design specification

Table A.1: Design specifications for the the winter simulation in EB-SILON®Professional

	Value	Unit
Furnace		
Air inlet	30, 1.01	[°C], [bar]
Air fan	1.06	[bar]
Air preheater	125	[°C]
Waste inlet	32, 17.54	[°C] [kg/s]
Air ratio	1.2	
Fly ash ratio	0.9	
NO-split	90	[%]
Exit flue gas	230	[°C]
Composition of waste		
C	29.8	[%]
H	4.2	[%]
O	15.4	[%]
N	0.6	[%]
S	0.2	[%]
Cl	0.6	[%]
H ₂ O in fuel	36.0	[%]
Ash	13.2	[%]
LHV	11.1	[MJ/kg]
Steam cycle		
Primary steam	400, 40, 74.0	[°C], [bar], [kg/s]
Steam turbine extraction 1	10	[bar]
Steam turbine extraction 2	3.5, 14.8	[bar], [kg/s]
Steam turbine outlet	1.2	[bar]
Condensate pump	11.8	[bar]
Feed water tank	140	[°C]

Continued on the next page

A. Design specification

DH cycle		
Condensor outlet	98.7	[°C]
Returned stream	38.9	[°C]
Pump	10.5	[bar]
HX to condensing reactor	44.3	[°C]
Heat pumps	61.0	[°C]
HX to economizer	73.6	[°C]
HX to cooling tower	73.6	[°C]
Hot water cycle		
HX to DH	108.1	[°C]
Pump	17	[bar]
Economizer (water side)	120	[kg/s]
Economizer (flue gas side)	150	[°C]
Cooling	128.3	[°C]

Table A.2: Design specifications for the the summer simulation in EB-SILON®Professional

	Value	Unit
Furnace		
Waste inlet	13.39	[kg/s]
DH cycle		
Condensor outlet	103.7	[°C]
Returned stream	49.8	[°C]
Pump	8.65	[bar]
HX to condensing reactor	52	[°C]
Heat pumps	67.1	[°C]
HX to economizer	77.48	[°C]
HX to cooling tower	70	[°C]

Table A.3: Flue gas input composition for the capture process in Aspen, collected from process data for the selected hour during winter and summer operation

	Winter	Summer	Unit
N ₂	77.40	72.49	[mol%]
CO ₂	11.33	11.26	[mol%]
H ₂ O	4.76	7.74	[mol%]
O ₂	6.51	8.50	[mol%]
CO	0.00000600	0.0000658	[mol%]

Table A.4: Design specifications for the capture processes in Aspen

	MEA	HPC	Unit
Sorbent concentration	30	30	[wt%]
Capture rate	90	90	[%]
Absorber inlet temperature	40	114	[°C]
Absorber pressure	1.06	7	[bar]
Desorber pressure	1.9	1.2	[bar]
Lean loading	0.25	-	[mol/mol]
Absorber height		20	[m]
Desorber height		10	[m]
Washer height	2	-	[m]
Adiabatic efficiency		95	[%]
Mechanical efficiency		85	[%]

B

Aspen PLUS simulation output

Figure B.1 and B.1 shows the model set up in Aspen PLUS for the CO₂ capture process utilizing MEA and HPC respectively. Figure B.3 shows the model set up in Aspen for the liquefaction process, this set up followed for both capture process.

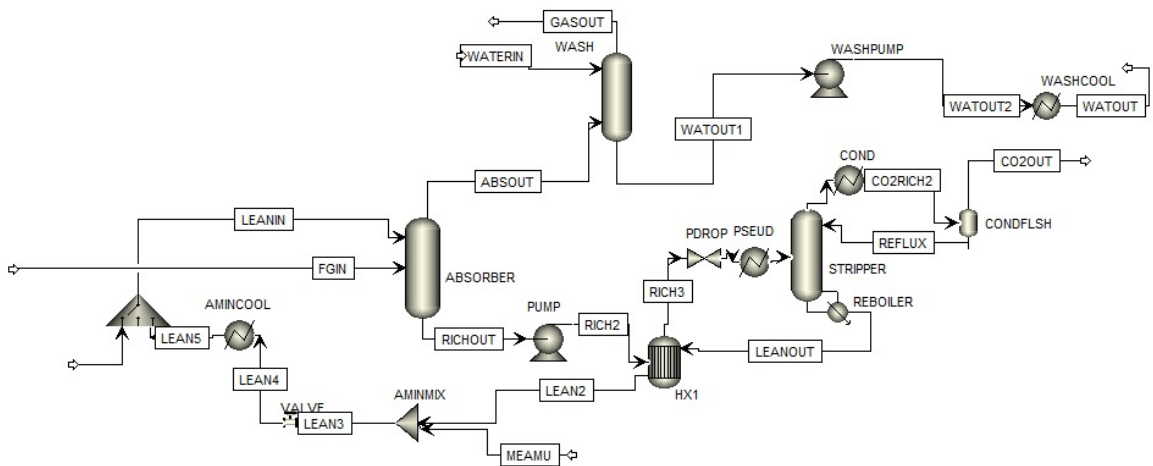


Figure B.1: Aspen PLUS model of the simulated MEA process

B. Aspen PLUS simulation output

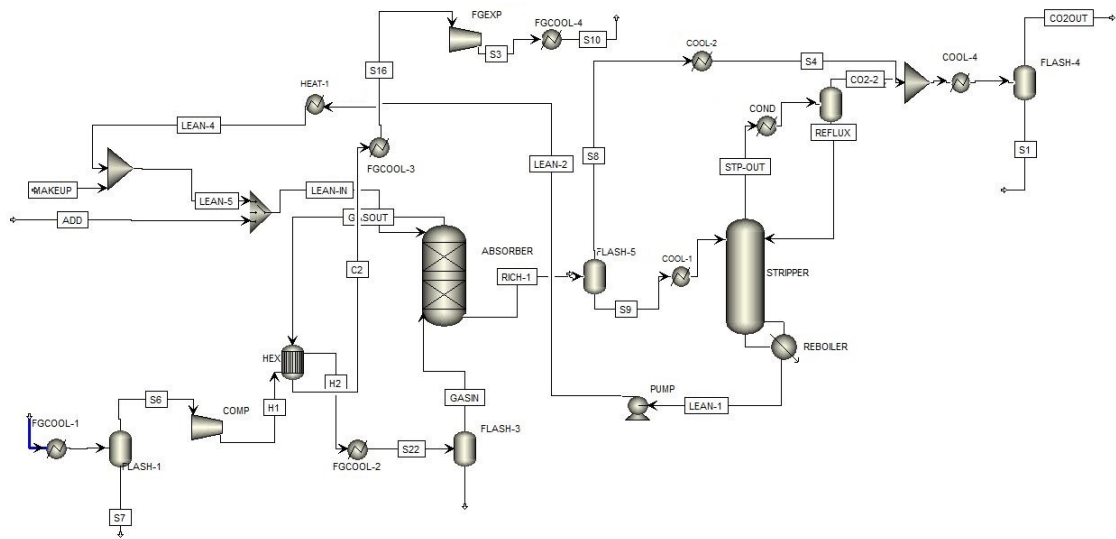


Figure B.2: Aspen PLUS model of the simulated HPC process

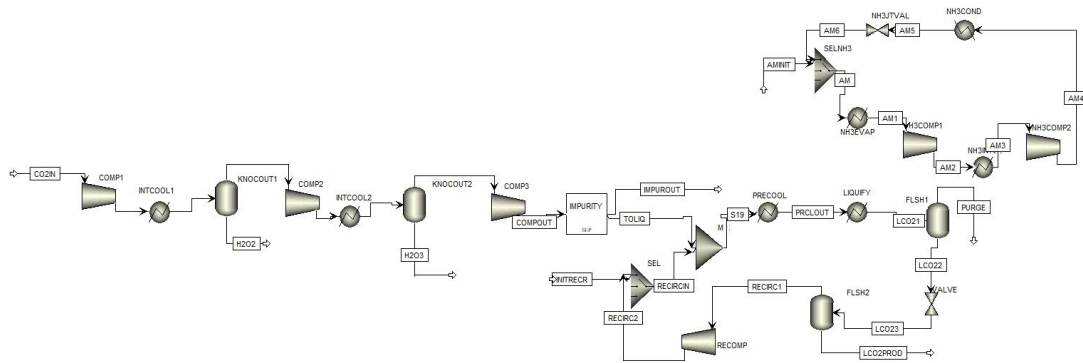


Figure B.3: Aspen PLUS model of the simulated compression and liquefaction process

Table B.1 and B.2 presents the performance of the in the CO₂ capture and liquefaction utilizing MEA and HPC as solvent from the simulation in Aspen PLUS. Table B.2 also contains the performance of a heater, for the pinch analysis was this heat demand summed to be fulfill internally by the cooler called FGCOOL-1.

Table B.1: Performance of the coolers in the CO₂ capture and liquefaction plant utilizing MEA as absorber for summer and winter operation

Unit	Winter			Summer		
	T _{start} [°C]	T _{target} [°C]	Q [MW]	T _{start} [°C]	T _{target} [°C]	Q [MW]
AMINCOOL	52.5	40.0	9.00	57.1	40.0	11.36
WASHCOOL	47.2	40.0	15.32	49.3	40.0	14.25
COND	107.3	20.0	21.12	107.5	35	18.96
INTERCOOL1	90.1	20.0	0.71	104.1	35.0	0.76
INTERCOOL2	94.3	20.0	0.70	111.4	35.0	0.70
PRECOOL	88.5	20.0	0.76	103.8	35.0	0.70
NH3COND	89.1	20.2	3.90	129.2	35.5	4.03
NH3INTCOOL	68.5	20.0	0.30	88.9	35.0	0.35

Table B.2: Performance of the coolers and one heater in the CO₂ capture and liquefaction plant utilizing HPC as absorber for summer and winter operation

Unit	Winter			Summer		
	T _{start} [°C]	T _{target} [°C]	Q [MW]	T _{start} [°C]	T _{target} [°C]	Q [MW]
FGCOOL-1	160.0	31.7	8.59	160.0	44.3	7.16
FGCOOL-2	124.3	120.0	14.30	130.0	120.0	0.60
FGCOOL-3	-	-	0.00	-	-	0.00
FGCOOL-4	89.2	20.0	25.18	103.3	35.0	20.60
HEAT-1	112.1	115.0	2.05	112.4	115.0	1.71
COOL-1	-	-	0.00	-	-	0.00
COOL-2	100.7	20.0	2.38	102.3	35.0	3.17
COND	96.3	20.0	26.90	97.3	35	26.10
INTCOOL1	107.7	20.0	0.84	111.7	35.0	0.71
INTCOOL2	101.3	20.0	0.88	111.0	35.0	0.72
NH3COND	89.1	20.2	3.87	129.2	35.5	4.02
NH3INTCOOL	68.5	20.0	0.30	88.9	35.0	0.35
PRECOOL	100.7	20.0	0.90	103.8	35.0	0.70

C

Estimation of power demand for air coolers

This chapter describes the calculation regarding the power needed for air coolers. The calculations and design specification, presented in Table C.1, are based on the works on Towler and Sinnott [44]. The fan work W_f is calculated with Equation C.1-C.4, where U is assumed to be $0.375 \text{ kW/m}^2\text{K}$, ΔT_{lm} is assumed 14K and F_t is assumed 0.85 .

$$A = \frac{Q}{U\Delta T_{lm}F_t} \quad (\text{C.1})$$

$$N_b = \frac{A}{A_t N_{bd} N_{bk}} \quad (\text{C.2})$$

$$A_b = l_t p_t N_{bk} \quad (\text{C.3})$$

$$W_f = \frac{u_f A_b \Delta P_b N_b}{\eta_f \eta_m} \quad (\text{C.4})$$

Table C.1: Design specification of air cooler

Tube length	l_t	12	[m]
Tube area	A_t	0.958	[m ²]
Banks/bundle	N_{bd}	6	
Tubes/bank	N_{bk}	44.0	
Tube pitch	p_t	0.0635	[m]
Pressure loss over bundle	ΔP_b	150	[N/m ²]
Face velocity	u_f	2.50	[m/s]
Fan efficiency	η_f	0.70	
Motor efficiency	η_m	0.9	

DEPARTMENT OF SOME SUBJECT OR TECHNOLOGY
CHALMERS UNIVERSITY OF TECHNOLOGY
Gothenburg, Sweden
www.chalmers.se



CHALMERS
UNIVERSITY OF TECHNOLOGY